



Natural Resources
Canada

Ressources naturelles
Canada

**GEOLOGICAL SURVEY OF CANADA
OPEN FILE 9161**

**Rhenium-rich molybdenite and Re-Os age of the Archean
porphyry-style Don Rouyn deposit, Abitibi greenstone
belt, Rouyn-Noranda, Quebec**

P. Mercier-Langevin, R.A. Creaser, J. Goutier, and I. Kjarsgaard

2024

Canada

**GEOLOGICAL SURVEY OF CANADA
OPEN FILE 9161**

Rhenium-rich molybdenite and Re-Os age of the Archean porphyry-style Don Rouyn deposit, Abitibi greenstone belt, Rouyn-Noranda, Quebec

P. Mercier-Langevin¹, R.A. Creaser², J. Goutier³, and I. Kjarsgaard⁴

¹Geological Survey of Canada, 490, rue de la Couronne, Québec, Quebec

²University of Alberta, 116th Street and 85th Avenue, Edmonton, Alberta

³Retired, Rouyn-Noranda, Quebec

⁴Consulting mineralogist, 15 Scotia Place, Ottawa, Ontario

2024

© His Majesty the King in Right of Canada, as represented by the Minister of Natural Resources, 2024

Information contained in this publication or product may be reproduced, in part or in whole, and by any means, for personal or public non-commercial purposes, without charge or further permission, unless otherwise specified.

You are asked to:

- exercise due diligence in ensuring the accuracy of the materials reproduced;
- indicate the complete title of the materials reproduced, and the name of the author organization; and
- indicate that the reproduction is a copy of an official work that is published by Natural Resources Canada (NRCan) and that the reproduction has not been produced in affiliation with, or with the endorsement of, NRCan.

Commercial reproduction and distribution is prohibited except with written permission from NRCan. For more information, contact NRCan at copyright-droitdauteur@nrcan-rncan.gc.ca.

Permanent link: <https://doi.org/10.4095/332556>

This publication is available for free download through GEOSCAN (<https://geoscan.nrcan.gc.ca/>).

Recommended citation

Mercier-Langevin, P., Creaser, R.A., Goutier, J., and Kjarsgaard, I., 2024. Rhenium-rich molybdenite and Re-Os age of the Archean porphyry-style Don Rouyn deposit, Abitibi greenstone belt, Rouyn-Noranda, Quebec; Geological Survey of Canada, Open File 9161, 31 p. <https://doi.org/10.4095/332556>

Publications in this series have not been edited; they are released as submitted by the author.

ISSN 2816-7155
ISBN 978-0-660-69886-1
Catalogue No. M183-2/9161E-PDF

Rhenium-rich molybdenite and Re-Os age of the Archean porphyry-style Don Rouyn deposit, Abitibi greenstone belt, Rouyn-Noranda, Quebec

Patrick Mercier-Langevin^{1*}, Robert A. Creaser², Jean Goutier³, and Ingrid Kjarsgaard⁴

¹Geological Survey of Canada, 490 rue de la Couronne, Québec, Quebec G1K 9A9

²University of Alberta, 116th Street and 85th Avenue, Edmonton, Alberta T6G 2R3

³Retired, Rouyn-Noranda, Quebec J9X 1M8

⁴Consulting mineralogist, 15 Scotia Place, Ottawa, Ontario, Canada K1S 0W2

*Corresponding author email: patrick.mercier-langevin@rncan-nrcan.gc.ca

ABSTRACT

This report presents Re-Os dating of molybdenite from the Don Rouyn deposit and St. Jude breccia prospect in the Rouyn-Noranda mining district in the southern Abitibi greenstone belt, Quebec. Both have been described as porphyry-style, magmatic-hydrothermal Cu-(Au-Mo) deposits associated with the Flavrian and Powell subvolcanic plutons based on the nature of the mineralized zones, their setting and available U-Pb age constraints. To further constrain the timing of mineralization, molybdenite was sampled at both sites for Re-Os geochronology. Although the analyzed sample from the St. Jude prospect did not yield a realistic age, a molybdenite mineral separate sample from the Don Rouyn deposit yielded a reliable age of 2689 ± 11 Ma. Interestingly, the Don Rouyn molybdenite is distinguished by extremely high Re content (>5200 ppm Re) that compares with that of the world's richest porphyry deposits.

Based on the Re-Os age obtained in this study and limited descriptions of the deposit available in the literature, the Don Rouyn deposit is most likely associated with the emplacement of the Flavrian-Powell intrusive complex at ~ 2700 Ma, as suggested in previous studies. However, a younger timing of emplacement, comparable to other ca. 2682-2680 sub-alkaline to alkaline magmatic-hydrothermal Cu-(Au-Mo) deposits in the southern part of Blake River Group, although less likely, cannot be entirely ruled out based on the available constraints and the molybdenite Re-Os age presented here.

INTRODUCTION

The Abitibi greenstone belt is host to various types and styles of ore deposits. Gold is the main metal of the belt, though Cu, Zn, Ni and Ag are also very important from an economic standpoint. Other significant metals and substances have been or are being extracted (for example platinum group elements, Pb, Li, Fe, Mo, Se and Bi). Gold deposits of the belt are predominantly of the orogenic type (Dubé and Mercier-Langevin, 2020) whereas base metals are dominantly from volcanogenic massive sulphide deposits, with several other types of precious, base and trace metal deposits. Although not very common, Archean porphyry-style deposits have been described in the Superior Province and Abitibi belt (e.g., Côté Gold deposit: Katz et al., 2017, 2021; Chibougamau camp: Côté-Mantha et al., 2012; Leclerc et al., 2012; Troilus Au(-Cu) deposit: Fraser, 1993). It also includes the Don Rouyn Cu(-Au-Mo) deposit in the Rouyn-Noranda district, which has been

explored as a gold prospect in the early years (Wilson, 1941; Dresser and Denis, 1949) and later considered an Archean porphyry-type deposit (Kirkham, 1972; Goldie et al., 1979; Jébrak et al., 1996; Sinclair et al., 2016). It also includes a nearby Cu-Mo-Au prospect (St. Jude) that is also considered to be the product of a magmatic-hydrothermal system (Kennedy, 1981, 1985; Carrier, 1992; Pelletier and Couture, 1996; Galley and van Breemen, 2002). Understanding the timing and style of mineralization is key to recognizing such deposits and suggesting a possible affiliation with intrusive rocks and porphyry-style, magmatic-hydrothermal systems.

This report presents Re-Os geochronological results from negative-thermal ionization mass spectrometry (N-TIMS) dating of molybdenite from the Don Rouyn deposit and St. Jude breccia prospect in the Rouyn-Noranda mining district, southern Abitibi greenstone belt, Superior Province, Québec. The dated samples are associated with Cu-Mo-Au mineralization and, in one case (Don Rouyn), provide constraints on the timing of porphyry-style mineralization. The work presented here was initiated by the Geological Survey of Canada through the Targeted Geoscience Initiative (TGI) *Lode Gold* (TGI-4: Dubé and Mercier-Langevin, 2015) and *Gold* (TGI-5: Mercier-Langevin et al., 2020) projects using archive material from the Geological Survey of Canada and Géologie Québec, and with the available information from literature as mining at Don Rouyn stopped in 1980 and the open pit mine has since been flooded. This work was done in collaboration with the Ministère des Ressources naturelles et des Forêts and the University of Alberta. The objective of this study was to improve the current knowledge of intrusion-associated deposits by adding critical age constraints and help improve our understanding of the metallogenic evolution of the southern Abitibi greenstone belt. Geochronology results and their implications are reported and briefly discussed here.

Regional Geological Setting

The Superior Province consists of Mesoproterozoic to Neoproterozoic subprovinces of east-west and north-south dominant orientations assembled in the Neoproterozoic, forming the largest Archean craton of the planet (Simard et al., 2010; Percival et al., 2012). The Abitibi greenstone belt, located in the Southern part of the Superior Province, has a surface area of approximately 100 000 km² (maximal dimensions of about 720 km ENE-WSW by 200 to 260 km N-S: Fig. 1), and represents the largest extent of Neoproterozoic supracrustal rocks of the planet.

The Abitibi greenstone belt comprises several sequences of volcanic and sedimentary rocks generally oriented east-west, folded and intersected by several faults and intrusive bodies (Fig. 1). The primary characteristics of rocks are generally well preserved despite the deformation and the low to moderate metamorphism affecting the entire belt (Monecke et al., 2017a). Significant corridors of ductile to brittle faults intersect the belt from east to west (Poulsen, 2017). The principal elements of the Abitibi greenstone belt are described in detail in numerous publications and readers are referred to Dubé and Mercier-Langevin et al. (2020) for more information and a list of key references.

Over half of the surface of the Abitibi greenstone belt consists of intrusive rocks (Monecke et al., 2017a; Mercier-Langevin et al., 2022). These intrusive bodies, which are commonly polyphased, are present all over the belt (Fig. 1) and their age varies from about 2750 to 2640 Ma (Goutier and Melançon, 2010; Dubé and Mercier-Langevin, 2020). Their composition varies from ultramafic to

felsic and from subalkaline to alkaline (Dubé and Mercier-Langevin, 2020). Due to the association between intrusive rocks and the tectonic evolution of the belt, these are commonly grouped relative to their formation setting. A significant part of these intrusive rocks is “syn-volcanic” and grouped according to their main composition, either as ultramafic to mafic or intermediate to felsic. Post-volcanic intrusive rocks are grouped according to their age with respect to large sedimentary assemblages: syn-turbidites, and syn-fluvial-alluvial sedimentation (syn-Timiskaming in the southern Abitibi) while the more recent intrusive rocks are “post-Timiskaming” (Dubé and Mercier-Langevin, 2020). Syn-volcanic intrusive bodies represent a significant part of the exposed rocks of the Abitibi belt, while the post-Timiskaming ones represent slightly less than 10% (Dubé and Mercier-Langevin, 2020). Syn-volcanic intrusive rocks are sometimes associated with volcanogenic massive sulphide mineralization, with Cu-(Au-Mo) magmatic-hydrothermal mineralization and with Ni-Cu-(PGE)-Cr-V mineralization. Mathieu et al. (2020) further divided the large intrusive bodies of the Abitibi greenstone belt into tonalite-trondhjemite-granodiorite (TTG) and tonalite-trondhjemite-diorite (TTD) suites based on the main rock types present (granodiorite versus diorite) and petrogenesis, suggesting that magmatic-hydrothermal systems of the belt are preferentially associated with TTD suites that come from magmas with a stronger mantle component than TTG suites, whereas Meng et al. (2021) conclude that Archean magmas, whether oxidized or reduced, are amenable to porphyry-style deposits.

Local Geological Setting

Blake River Group

The Blake River Group is the youngest and richest volcanic sequence of the Abitibi greenstone belt and is known for its major endowment in VMS deposits (Mercier-Langevin et al., 2011). The Blake River Group consists of several submarine volcanic and volcanoclastic sequences. The volcanic rocks are predominantly bimodal in composition (basalt, basaltic andesite and andesite, and rhyodacite and rhyolite). The Blake River Group is locally unconformably overlain by the polymictic conglomerates and alkalic volcanic rocks of the Timiskaming Group, and by the Paleoproterozoic conglomerates of the Cobalt Group. Some Archean syn-volcanic (gabbro, diorite, tonalite, e.g.: Flavrian and Powell plutons: Fig. 2) and syn-tectonic intrusions (syenite, diorite, granodiorite, granite) cut the Blake River Group volcanic rocks. In Québec, the Blake River Group is bounded by two major fault zones: the Porcupine-Destor fault zone to the north, and the Cadillac fault zone to the south (Fig. 1). Rocks of the Blake River Group were subjected to major north-south shortening events. However, the deformation is heterogeneously distributed within the Blake River Group; the central part is characterized by tilting of the strata and by the presence of major folds, whereas the northern and southern margins are characterized by the presence of laterally extensive shears and tight folds. The Blake River Group rocks are affected by lower greenschist (north) to lower amphibolite (south) grade metamorphism (Jolly, 1978; Dimroth et al., 1983; Powell et al., 1995).

Flavrian and Powell plutons

The Flavrian and Powell plutons were emplaced within the central part of the Blake River Group and underly most of the Noranda central camp VMS deposits (Fig. 2). These subvolcanic plutons are comagmatic with the host volcanic succession (Goldie, 1976; Kennedy, 1984; Paradis et al.,

1988). It is also coeval with the host volcanic rocks with U-Pb zircon ages of $2700.8 \pm 2.6/-1.0$ Ma (Mortensen, 1993), $2700 \pm 3/-2$ Ma (youngest trondhjemite intrusion in central part of the complex) and 2697 ± 2 Ma (aplite: Galley and van Breemen, 2002). The latter two ages were refined by McNicoll et al. (2014) who obtained an age of 2700.7 ± 0.6 Ma for the trondhjemite and an age of 2696.6 ± 0.9 Ma for the aplite. McNicoll et al. (2014) also dated the Powell pluton (main trondhjemite phase) a few hundred meters south-west of the former Don Rouyn mine and obtained an age of 2700.1 ± 1.0 Ma.

The Flavrian pluton consists of an early quartz-diorite phase cut by tonalite sills that were in turn intruded by trondhjemite sills (Kennedy, 1984; Richard, 1999). These early tonalite and trondhjemite phases, which represent about a third of the pluton, were intruded by diorite (“Eldrich” phase) and a younger trondhjemite stock in the central part of the intrusion (late trondhjemite core). Aphyric to porphyritic trondhjemitic dyke swarms cut the pluton in its southern part and a felsic porphyry dyke swarm intruded the western margin of the complex. Late diorite dykes cut all previous phases (Galley and van Breemen, 2002). The early phases (tonalite and early trondhjemite) of the Flavrian pluton predate the volcanogenic massive sulphide deposits of the Noranda central camp and show evidence of high-temperature hydrothermal alteration (Cathles, 1993; Kennedy, 1984; Galley and van Breemen, 2002; Taylor et al., 2014), whereas the later phases such as the late trondhjemite core is devoid of such hydrothermal alteration, although associated with metasomatic devolatilization as shown by the biotite-amphibole-apatite-sulphide reaction halo around it (Galley and van Breemen, 2002), which may have been favourable for the development of porphyry-style mineralization at ≤ 2700 Ma.

Don Rouyn deposit

The Don Rouyn deposit, primarily mined in an open pit operation as Cu-rich siliceous flux for the Horne smelter between 1957 and 1980, is located a few kilometers east of downtown Rouyn-Noranda (Fig. 2). Goldie (1976) mentioned that reserves were about 36 Mt at an estimated grade of 0.15 % Cu. The deposit has not been systematically mapped in detail although metal distribution and ore envelopes are shown in Goldie et al. (1979) and Jébrak et al. (1996). The deposit is hosted in the Powell pluton (Figs. 2, 3), which is massive to weakly foliated and contains medium-grained anhedral quartz and plagioclase with interstitial chlorite and epidote, with minor amounts of sericite and calcite (Fig. 4A). The Powell pluton is bounded to the north and south by the Beauchatel and Horne Creek faults, respectively. The unit has been described as a peraluminous, tholeiitic tonalite (e.g., Jébrak et al., 1996), whereas one sample analyzed for this project is strongly altered and plots as an alkaline rock (Fig. 5A; Table 2). This sample, however, has a rare earth elements pattern typical of the Flavrian and Powell rocks excepts for the Eu anomaly that is not present in the analyzed samples, perhaps because of the alteration that affects the feldspars (Fig. 5B). The geochemical signature of the Powell pluton sample dated in McNicoll et al. (2014) was plotted in figure 5B as well for comparison, which has much higher rare earth-elements concentrations. Unaltered and altered samples from the Don Rouyn mine host intrusive rocks (Jébrak and Harnois, unpublished data) dominantly plot in the granite field (Fig. 5A). The tonalite-trondhjemite at the mine is cut by numerous altered but barren WSW-ENE mafic dykes (Figs. 3B, 4B) and the mineralized zones are bounded to the south by a large diorite dyke.

The mineralized zones consist of a few tens of meters wide bornite-, chalcopyrite-, pyrite- and molybdenite-bearing core zone surrounded by a somewhat WSW-ENE-oriented 50 to 100 m-wide elongated chalcopyrite, pyrite \pm molybdenite halo, and a poorly defined external pyrite \pm chalcopyrite zone (Fig. 3). Hydrothermal alteration consists of chlorite, albite, epidote, carbonate and sericite (Fig. 6) primarily developed at the expense of primary feldspar and ferro-magnesian minerals (biotite and/or amphibole). Primary textures are generally well to partly preserved (Fig. 7A), except where chlorite alteration is more intense, and where foliation is well developed and overprints alteration and mineralization (Fig. 7B). The mineralized zones are also cut by late, syn-main deformation white quartz veins (Fig. 8A). The chlorite-epidote-albite-calcite alteration is locally associated with disseminated hematite (Fig. 8B), especially in the pyrite \pm chalcopyrite zone (Jébrak et al., 1996). In mineralized samples, quartz, albite, chlorite, sericite and calcite are the main minerals (Table 3), although a long list of trace minerals is also present as detailed in Table 3.

The sulphides are generally finely disseminated (≤ 5 vol. %) in the matrix and closely associated with chlorite (Figs. 6B, 7A, 8A, and 9A). Bornite, which is only present in the core zone (Fig. 3), is irregular and generally very fine-grained, in association with chalcopyrite (Fig. 9B). Trace amounts of digenite and covellite are locally associated with the bornite (Table 3). Molybdenite more commonly forms thin veins in the core zone (Fig. 10A, B), or is associated with chalcopyrite-rich bands where it forms coarse-grained flakes (Fig. 11A, B). Gold is present in traces as tiny electrum inclusions in pyrite in the Cu-rich zones (Table 3). Anomalous gold grades spatially coincide with elevated Cu and Mo grades (Jébrak et al., 1996).

St. Jude breccia

The St. Jude breccia and the Sylvie showing have been described and mapped in detail in Kennedy (1981, 1984), Carrier (1992), Pelletier and Couture (1996) and Galley and van Breemen (2002). Mineralized zones consist of pyrite-chalcopyrite-bornite-molybdenite-mineralized areas hosted in an intrusive breccia body located in the western margin of the Flavrian pluton (Fig. 2). The breccia is polyphased and hosted in the early trondhjemite but is associated with a trondhjemitic core that strongly resemble the late trondhjemite in the central part of the Flavrian and Powell plutons. Pyrite, sphalerite and galena are present outward from the Cu-Mo-Au core of the breccia pipe. The central part of the mineralized area (Sylvie showing) is biotite-altered (potassic alteration) and transitions in a sericite-dominated (phyllic alteration) assemblage outward. The breccia units are cut by a molybdenite-bearing quartz vein that is in turn cut by an aphyric aplitic dyke. Mineralization is ≤ 2700 Ma and ≥ 2697 Ma based on the ages of the host trondhjemite and crosscutting aplite dyke (Galley and van Breemen, 2002; McNicoll et al., 2014).

Re-Os GEOCHRONOLOGY

Sample Selection

Two samples were selected to better constrain the timing of porphyry-style mineralization in the Flavrian and Powell plutons. The first sample (JH-98-DR) comes from the former Don Rouyn mine and its central, Cu-rich zone (Figs. 2, 3: UTM NAD83, zone 17: 643 460 m E, 5 345 990 m N (± 20 m)). Sample JH-98-DR, which is from the GSC archives in Ottawa, is cut by a 1–2.5 cm-

wide sulphide vein containing abundant, relatively coarse-grained molybdenite (Fig. 11), chalcopyrite, pyrite and traces of bornite in an albite-sericite-chlorite-calcite-altered tonalite, although the dated sample is from a disseminated molybdenite-bearing part of the sample (Fig. 11A inset).

The second sample (“St Jude”) was taken at surface at the Sylvie Cu-Mo-Au prospect (UTM NAD 83, zone 17: 631 700 m E, 5 352 151 m N) and represents a molybdenite-coated fracture (Fig. 12) cutting across nested breccia intrusive units and syn-volcanic porphyry and granophyric dykes (*see* figure 4 *in* Galley and van Breemen, 2002). Although relatively fresh overall, the sample was taken on surface in a slightly oxidized area.

Re-Os Analytical Methods

Metal-free crushing followed by gravity and magnetic concentration was used to obtain molybdenite mineral separates. Methods used for molybdenite analysis are described in detail in Selby and Creaser (2004) and Markey et al. (2007). The ^{187}Re and ^{187}Os concentrations in molybdenite were determined by isotope dilution mass spectrometry using Carius-tube, solvent extraction, anion chromatography and negative thermal ionization mass spectrometry (N-TIMS) techniques at the University of Alberta. For this work, a mixed double spike containing known amounts of isotopically enriched ^{185}Re , ^{190}Os , and ^{188}Os analysis was used (Markey et al., 2007). Isotopic measurements used a ThermoScientific Triton mass spectrometer with static faraday collectors. Total procedural blanks for Re and Os are less than <3 picograms and 2 picograms, respectively, which are insignificant in comparison to the Re and Os concentrations in molybdenite. The Chinese molybdenite powder HLP-5 (Markey et al., 1998) is routinely analyzed as a standard, and during the 2 years preceding the analyses of the sample from Don Rouyn, returned an average Re-Os date of 221.56 ± 0.40 Ma (1σ uncertainty, $n = 10$), identical to that reported in Markey et al. (1998) of 221.0 ± 1.0 Ma. The ^{187}Re decay constant ($\lambda^{187}\text{Re}$) used for age calculation is $1.666 \pm 0.005 \times 10^{-11} \text{ a}^{-1}$ (Smoliar et al., 1996), a value which is cross-calibrated to the U-Pb system (^{238}U and ^{235}U) to better than $\sim \pm 0.31\%$ (Selby et al., 2007).

Re-Os Analytical Results

The results of the Re-Os age determinations are presented in Table 1. The age uncertainty is quoted at 2σ level, and includes all known analytical uncertainty, including a $\sim 0.31\%$ uncertainty in the decay constant of ^{187}Re . Age uncertainties are listed both to include the ^{187}Re decay constant uncertainty, for when comparison to isotopic dates using other isotope systems is required (such as U-Pb), and without the decay constant uncertainty, for use only when comparing Re-Os dates to Re-Os dates.

Sample JH-98-DR (Don Rouyn) yielded enough molybdenite mineral separate for a single analysis (5 mg) with an age of 2689 ± 7 (± 11 Ma if available U-Pb constraints considered), which is considered a reliable analysis. Interestingly, the sample is distinguished by extremely high Re content (>5000 ppm Re).

The St. Jude sample produced a large mineral separate, but the Re content of molybdenite was found to be very low (<1.5 ppm). An initial analysis yielded an age of 2789 ± 12 Ma (± 7 Ma if

comparing with Re-Os ages only) and a replicate at 2771 ± 12 Ma. This level of reproducibility from a molybdenite mineral separate is not ideal, and likely indicates the sample has suffered significant “decoupling” of radiogenic ^{187}Os from Re inside the crystal (see Selby and Creaser, 2004). This effect can lead to inaccurate and irreproducible ages from the same mineral separate, if the amounts of sample analyzed are not enough to overcome the sample heterogeneity. Typically, molybdenite sample aliquots weights of >5 mg overcome this effect, but with the St. Jude sample, replicates of ~ 35 mg did not reproduce their age (2789 and 2771 Ma, both ± 7 Ma when comparing Re-Os ages to Re-Os ages). As such, a third replicate with half the sample weight was undertaken and yielded a much younger age of $2648 \pm 7/12$ Ma, clearly indicating very strong age heterogeneity (Re-Os decoupling) for this sample (Table 1). A fourth analysis was made using all remaining molybdenite (107 mg), which yielded an age of $2720 \pm 7/11$ Ma. Given the age heterogeneity effect generally decreases with sample aliquot size, the fourth replicate age of $2720 \pm 7/11$ Ma is likely closest to the true formation age of the molybdenite, but given the large heterogeneity for this sample, extreme caution has to be used for geological interpretation of this age. Moreover, as discussed below, a 2720 Ma age for the mineralization is geologically not realistic given the much younger age of the host rocks.

DISCUSSION

The Re-Os molybdenite age from the Don Rouyn deposit ($2689 \pm 7/11$ Ma) is in agreement, within error, with previous interpretations indicating that the Cu(-Mo-Au) mineralization in the 2700 Ma Powell intrusion might be syn-magmatic (e.g., Kirkham, 1972; Goldie et al., 1979), which would confirm the magmatic-hydrothermal, and porphyry-like nature of the deposit.

However, although plausibly as old as ~ 2700 Ma, the deposit could also be as young as ~ 2678 Ma as per the 11 Ma Re-Os molybdenite age uncertainty (Table 1). In the southern Abitibi the 2700–2678 Ma period marks the transition from major volcanism to thick turbiditic sedimentation and early regional thin-skin deformation, and a transition from sub-alkaline, tholeiitic and calc-alkaline magmatism to more alkaline/shoshonitic magmatism at belt scale (Dubé and Mercier-Langevin, 2020). Syn-magmatic, or magmatic-hydrothermal Au-Cu-(\pm Mo) deposits associated with sub-alkaline to alkaline intrusions are known in the region, including: the Upper Beaver deposit, dated at 2680 Ma (Re-Os on molybdenite: Kontak et al., 2013; Mercier-Langevin et al., 2021; Dubé et al., in preparation); the Croxall Cu-Mo-Au porphyry-style prospect in the Clifford stock, dated at 2682.4 ± 7.8 Ma (Re-Os on molybdenite: Piercey et al., 2008); and the Baie Renault Au-Cu-Mo-Ag \pm Pb prospect, dated at ≤ 2682 Ma (U-Pb age of host syenite: David et al., 2011). In each case, the polymetallic mineralized zones are considered to be of magmatic-hydrothermal origin and associated with the magmatic rocks that host or are spatially associated with the sulphides. The presence of numerous such ca. 2682–2680 Ma Cu-Mo-Au deposits and prospects in the southern Blake River Group could suggest that the Don Rouyn deposit is part of that metallogenic event and, therefore, perhaps significantly younger (10–20 m.y.) than its host rocks (Powell pluton at 2700 Ma). However, despite the common occurrence of alkaline rocks in the southern Abitibi and southern Blake River Group, no alkaline/shoshonitic rocks are present at the Don Rouyn deposit or in its immediate vicinity, which does not preclude the possibility of such intrusive rocks being present at depth, but so far, no evidence would suggest so. Also, the concentric sulphide assemblages and metal zonation at Don Rouyn is compatible with an early origin for the Cu(-Au-Mo) mineralization. Moreover, the mineralized zones are cut by a series of mafic dykes that are

altered and locally mineralized and, although not dated, considered to be syn-volcanic and feeders of the basaltic and andesitic volcanic units in the area (Goldie et al., 1979), which would also indicate an early origin for the mineralization. Therefore, the Don Rouyn deposit is most likely associated with the emplacement of the Flavrian and Powell plutons at ~2700 Ma as previously suggested, but a younger timing of emplacement, comparable to other ~2682–2680 magmatic-hydrothermal Cu(-Au-Mo) in the southern Blake River Group, cannot be entirely ruled out based on the available constraints and the molybdenite Re-Os age presented here.

Interestingly, the Re content in the dated molybdenite (5228 ppm: Table 1) is very high. Compared with other molybdenite-bearing porphyry-type deposits of the world, the Don Rouyn molybdenite sample plots amongst the richest molybdenites (Fig. 13). Although more analyses would be necessary to complete a rigorous comparison, the results obtained in this study indicate that Don Rouyn molybdenite compares with that present in the richest Cu-Au porphyry systems, which appear to be slightly richer than Cu and Cu-Mo porphyry systems based on Sinclair et al. (2016) data (Fig. 13). It would be interesting to confirm those results and study the reasons why Don Rouyn is, perhaps, enriched in Re compared to other porphyry systems, and other Archean molybdenite-bearing deposits (e.g., Upper Beaver deposit molybdenite with 155–166 ppm Re: Mercier-Langevin et al., 2021; Côté Gold deposit molybdenite with 334–342 ppm Re: Katz et al., 2021; Kirkland Lake molybdenite with 0.5–1 ppm Re: Ispolatov et al., 2008).

The sample from the St. Jude prospect unfortunately did not yield reliable results. Replicate analyses indicate strong heterogeneity in the dated molybdenite, and the dates that were obtained are geologically impossible as they are much older than the host rocks that are ~2700 Ma. The age of the Cu-Mo-Au mineralization at St. Jude has however been constrained at 2700–2697 Ma by crosscutting relationships and U-Pb zircon geochronology (Galley and van Breemen, 2002; McNicoll et al., 2014).

CONCLUSION

The formation (and/or preservation) of porphyry-*type* mineralization in the Archean is a topic of debate (e.g., Meng et al., 2021), but there is mounting evidence that magmatic-hydrothermal deposits of different ages and contexts are present in Archean settings such as the southern Abitibi greenstone belt, with numerous examples exhibiting porphyry-*style* features (e.g., Mercier-Langevin et al., 2012 and references therein). Although this may seem a philosophical discussion, implications for exploration and the understanding of metallogenic processes are very important as over half of the Abitibi belt consists of intrusive rocks, and other areas of the Superior Province have an even higher proportion of intrusive rocks.

The timing and style of mineralization are key to recognizing the possible affiliation with porphyry-*style* or magmatic-hydrothermal type deposits. This report presents Re-Os geochronological results from N-TIMS dating of molybdenite from the Don Rouyn deposit and St. Jude breccia prospect in the Rouyn-Noranda mining district, southern Abitibi greenstone belt, Superior Province, Québec, which were both interpreted as porphyry-*style* mineralization associated with the ~2700–2697 Ma Flavrian and Powell subvolcanic plutons. The St. Jude prospect sample did not yield a geologically realistic age. However, the Don Rouyn deposit sample yielded a reliable age of $2689 \pm 7/11$ Ma. Interestingly, the Don Rouyn molybdenite is

distinguished by extremely high Re content (>5200 ppm Re) that compares with that of the richest porphyry deposits.

Based on the Re-Os age obtained in this study, the Don Rouyn deposit is most likely associated with the emplacement of the Flavrian and Powell plutons at ~2700 Ma, as suggested in previous studies. However, a younger timing of emplacement, comparable to other ~2682–2680 sub-alkaline to alkaline intrusion-associated magmatic-hydrothermal Au-Cu-(±Mo) deposits in the southern part of Blake River Group such as Upper Beaver, Croxall (Clifford) and Baie Renault, although less likely, cannot be entirely ruled out based on the available constraints and the molybdenite Re-Os age presented here. Further work would be necessary to fully understand the nature of the Don Rouyn deposit, and to confirm and explain the very high-Re content of the analyzed molybdenite.

ACKNOWLEDGMENTS

This is a contribution to the “OS-3 – Orogenic gold deposits: A closer look at the diversity of types, styles and ages of gold deposits in greenstone belts” project of the Targeted Geoscience Initiative Program of the Geological Survey of Canada. The authors are most grateful to D. Sinclair and A. Galley for access to archive samples at the Geological Survey of Canada and for scientific support, and to M. Jébrak and L. Harnois from Université du Québec à Montréal for the authorization to use their unpublished whole-rock data from the Don Rouyn deposit host intrusive rocks. M. Boutin helped prepare some of the figures. Thanks to Daniel Coutts for his constructive review of an earlier version of the manuscript.

REFERENCES

- Carrier, A., 1992, Le porphyre à Au-Mo de Saint-Jude: Unpublished Activité de Synthèse report (B.Sc. thesis), Université du Québec à Montréal, Montréal, Canada, 62 p.
- Cathles, L.M., 1993, Oxygen isotope alteration in the Noranda mining district, Abitibi greenstone belt, Quebec: *Economic Geology*, v. 88, p. 1483–1511.
- Côté-Mantha, O., Daignault, R., Gaboury, D., Chartrand, F., and Pilote, P., 2012, Geology, alteration, and origin of Archean Au-Ag-Cu mineralization associated with the synvolcanic Chibougamau pluton: The Brosman prospect, Abitibi greenstone belt, Canada: *Economic Geology*, v. 107, p. 909–934.
- David, J., McNicoll, V., Simard, M., Bandyayera, D., Hammouche, H., Goutier, J., Pilote, P., Rhéaume, P., Leclerc, F., and Dion, C., 2011, Datations U-Pb effectuées dans les provinces du Supérieur et de Churchill en 2009-2010: Ministère des Ressources naturelles et de la Faune, RP 2011-02, 37 p.
- Dimroth, E., Imreh, L., Goulet, N., and Rocheleau, M., 1983, Evolution of the south-central part of the Archean Abitibi belt, Quebec. Part III: plutonic and metamorphic evolution and geotectonic model: *Canadian Journal of Earth Sciences*, v. 20, p. 1374–1388.

Dresser, J.A., and Denis, T.C., 1949, *Geology of Quebec*: Department of Mines, Quebec, Geological Report 20, 562 p.

Dubé, B., and Mercier-Langevin, P., 2015, Targeted Geoscience Initiative 4: Contributions to the understanding of Precambrian lode gold deposits and implications for exploration: Geological Survey of Canada Open File 7852, 293 p.

Dubé, B., and Mercier-Langevin, P., 2020, Gold deposits of the Archean Abitibi greenstone belt, Canada: Society of Economic Geologists, Special Publication 23, p. 669–708.

Dubé, B., Mercier-Langevin, P., Hamilton, M.A., Wodicka, N., McNicoll, V., Fontaine, A., and Kontak, D.J., U-Pb ID-TIMS zircon geochronology for selected Archean intrusive rocks associated with gold deposits of Québec and Ontario; Geological Survey of Canada, Open File, in preparation.

Fraser, R.J., 1993, The lac Troilus gold-copper deposit, northwestern Quebec: A possible Archean porphyry system: *Economic Geology*, v. 88, p. 1685–1699.

Galley, A.G., and van Breemen, O., 2002, Timing of synvolcanic magmatism in relation to base-metal mineralization, Rouyn-Noranda, Abitibi volcanic belt, Quebec: Geological Survey of Canada, Current Research 2002-F8, 9 p.

Goldie, R.J., 1976, The Flavrian and Powell plutons, Noranda area, Quebec: Unpublished Ph.D. thesis, Queen's University, Kingston, Canada, 355 p.

Goldie, R., Kotila, B., and Seward, D., 1979, The Don Rouyn mine: an Archean porphyry copper deposit near Noranda, Quebec: *Economic Geology*, v. 74, p. 1680–1684.

Goutier, J., and Melançon, M., 2010, *Compilation géologique de la Sous-province de l'Abitibi*: Ministère des Ressources naturelles et de la Faune, RP 2010-04, 1 p., 2 maps. English version available: RP 2010-04(A).

Ispolatov, V., Lafrance, B., Dubé, B., Creaser, R., and Hamilton, M., 2008, Geologic and structural setting of gold mineralization in the Kirkland Lake-Larder Lake gold belt, Ontario: *Economic Geology*, v. 103, p. 1309–1340.

Jébrak, M., Harnois, L., Carrier, A., and Lafrance, J., 1996, Le porphyre à Cu-Au de Don Rouyn: Ministère des Ressources naturelles, MB 96-06, p. 85–89.

Jolly, W.T., 1978, Metamorphic history of the Archean Abitibi belt: Survey of Canada, Paper 78-10, p. 63–77.

Katz, L.R., Kontak, D.J., Dubé, B., and McNicoll, V., 2017, The geology, petrology, and geochronology of the Archean Côté Gold large-tonnage, low-grade intrusion-related Au(–Cu) deposit, Swayze greenstone belt, Ontario, Canada: *Canadian Journal of Earth Sciences*, v. 54, p. 173–202.

Katz, L.R., Kontak, D.J., Dubé, B., McNicoll, V., Creaser, R., and Petrus, J.A., 2021, An Archean porphyry-type gold deposit: The Côté Gold Au(-Cu) deposit, Swayze greenstone belt, Superior Province, Ontario, Canada: *Economic Geology*, v. 116, p. 47–89.

Kennedy, L., 1981, Evaluation of the Flavrian property, Eldrich, St. Jude Breccia, Lac Lebrun, Elder, reconnaissance alteration relationships: Assessment report for Gouvernement du Québec, report MB 37038, 8 p., 10 maps.

Kennedy, L.P., 1984, The geology and geochemistry of the Archean Flavrian pluton, Noranda, Quebec: Unpublished Ph.D. thesis, University of Western Ontario, London, Canada, 469 p.

Kirkham, R. V., 1972, Geology of copper and molybdenum deposits: Canada Geol. Survey, Paper 72-1A, p. 82–87.

Kontak, D., Dubé, B., McNicoll, V., Creaser, R., and Kyser, K., 2013, The Upper Beaver Au-Cu deposit, Kirkland Lake, Ontario, Canada: An Archean IOCG analogue or just an intrusion-related iron oxide copper-gold deposit?: Geological Association of Canada-Mineralogical Association of Canada Annual Joint Meeting, Abstract Volume 36, p. 122.

Leclerc, F., Harris, L.B., Bédard, J.H., van Breemen, O., and Goulet, N., 2012, Structural and stratigraphic controls on magmatic, volcanogenic, and shear zone-hosted mineralization in the Chapais-Chibougamau mining camp, northeastern Abitibi, Canada: *Economic Geology*, v. 107, p. 963–989.

Markey, R.J., Stein, H.J., and Morgan, J.W., 1998, Highly precise Re-Os dating for molybdenite using alkaline fusion and NTIMS: *Talanta*, V. 45, p. 935–946.

Markey, R.J., Stein, H.J., Hannah, J.L., Selby, D., and Creaser, R.A., 2007, Standardizing Re-Os geochronology: A new molybdenite Reference Material (Henderson, USA) and the stoichiometry of Os salts: *Chemical Geology*, v. 244, p. 74–87.

Mathieu, L., Crépon, A., and Kontak, D.J., 2020, Tonalite-dominated magmatism in the Abitibi subprovince, Canada, and significance for Cu-Au magmatic-hydrothermal systems: *Minerals*, v. 10, paper 242.

McDonough, W.F., and Sun, S.S., 1995. The composition of the Earth: *Chemical Geology*, v. 120, p. 223-253.

McNicoll, V., Goutier, J., Dubé, B., Mercier-Langevin, P., Ross, P.-S., Dion, C., Monecke, T., Legault, M., Percival, J., and Gibson, H., 2014, U-Pb geochronology of the Blake River Group, Abitibi greenstone belt, Quebec, and implications for base metal exploration: *Economic Geology*, v. 109, p. 27–59.

Meng, X., Richards, J.P., Kontak, D.J., Simon, A.C., Kleinsasser, J.M., Marsh, J.H., Stern, R.A., and Jugo, P.J., 2021, Variable modes of formation for tonalite-trondhjemite-granodiorite-diorite

(TTG)-related porphyry-type Cu ± Au deposits in the Neoproterozoic southern Abitibi subprovince (Canada): Evidence from petrochronology and oxybarometry: *Journal of Petrology*, v. 62, p. 1–29.

Mercier-Langevin, P., Goutier, J., Ross, P.-S., McNicoll, V., Monecke, T., Dion, C., Dubé, B., Thurston, P., Bécu, V., Gibson, H., Hannington, M., and Galley, A., 2011, The Blake River Group of the Abitibi greenstone belt and its unique VMS and gold-rich VMS endowment: Geological Survey of Canada, Open File report 6869, 61 p.

Mercier-Langevin, P., Houlié, M.G., Dubé, B., Monecke, T., Hannington, M.D., Gibson, H.L., and Goutier, J., 2012, A special issue on Archean magmatism, volcanism and ore deposits: Part 1. Komatiite-associated Ni-Cu-(PGE) sulfide and greenstone-hosted Au deposits – Preface: *Economic Geology*, v. 107, p. 745–753.

Mercier-Langevin, P., Lawley, C.J.M., Castonguay, S., Dubé, B., Bleeker, W., Pinet, N., Bécu, V., Pilote, J.-L., Jackson, S.E., Wodicka, N., Honsberger, I.W., Davis, W.J., Petts, D.C., Yang, Z., Jautzy, J., et Lauzière, K., 2020, Targeted Geoscience Initiative 5, Gold Project: A summary of contributions to the understanding of Canadian gold systems : Geological Survey of Canada, Open File 8712, p. 1–30.

Mercier-Langevin, P., Creaser, R.A., Dubé, B., Dubé, J., Kontak, D.J., Sutton, J., and Côté-Mantha, O., 2021, Molybdenite Re-Os age of a gold-rich vein, Porphyry zone, Upper Beaver deposit, Abitibi greenstone belt, Ontario: Geological Survey of Canada, Open File 8789, 13 p.

Mercier-Langevin, P., Dubé, B., Houlié, M.G., Bécu, V., Sappin, A.-A., Pilote, J.-L., and Castonguay, S., 2022, Métallogénie de la ceinture de roches vertes de l’Abitibi, Canada: In S. Decrée (ed.), *Ressources Métalliques 2 Cadre Géodynamique et Exemples Remarquables dans le Monde, Série Sciences – Géosciences – Ressources Naturelles : la Recherche Fondamentale Appliquée*, ISTE Éditions, Londres, p. 61-134.

Middlemost, E.A.K., 1994, Naming materials in the magma/igneous rock system: *Earth-Sciences Reviews*, v. 37, p. 215–224.

Monecke, T., Mercier-Langevin, P., Dubé, B., and Frieman, B.M., 2017a, Geology of the Abitibi greenstone belt: *Reviews in Economic Geology*, v. 19, p. 7–49.

Monecke, T., Gibson, H.L., and Goutier, J., 2017b, Volcanogenic massive sulfide deposits of the Noranda camp: *Reviews in Economic Geology*, v. 19, p. 169–223.

Mortensen, J.K., 1993, U - Pb geochronology of the eastern Abitibi Subprovince. Part 2: Noranda - Kirkland Lake area: *Canadian Journal of Earth Sciences*, v., 30, p. 29–41.

Paradis, S., Ludden, J., and Gélinas, L., 1988, Evidence for contrasting compositional spectra in comagmatic intrusive and extrusive rocks of the late Archean Blake River Group, Abitibi, Quebec: *Canadian Journal of Earth Sciences*, v. 25, p. 134–144.

Pelletier, C., and Couture, J.-F., 1996, Géologie de la brèche de St-Jude: Ministère des Ressources naturelles, MB 96-06, p. 37–40.

Percival, J.A., Skulski, T., Sanborn-Barrie, M., Stott, G.M., Leclair, A.D., Corkery, M.T., and Boily, M., 2012, Geology and tectonic evolution of the Superior Province, Canada: Geological Association of Canada Special Paper 49, p. 321–378.

Piercey, S. J., Chaloux, E.C., Péloquin, A.S., Hamilton, M.A., and Creaser, R.A., 2008, Synvolcanic and younger plutonic rocks from the Blake River Group: Implications for regional metallogenesis: *Economic Geology*, v. 103, p. 1243–1268.

Poulsen, K.H., 2017, The Larder Lake-Cadillac break and its gold districts: *Reviews in Economic Geology*, v. 19, p. 133–167.

Powell, W.G., Carmichael, D.M., and Hodgson, C.J., 1995, Conditions and timing of metamorphism in the southern Abitibi greenstone belt, Quebec: *Canadian Journal of Earth Sciences*; v. 32, p. 787–805.

Richard, M.G., 1999, Evolution of the Flavrian pluton and its association with the VHMS deposits and granitoid-hosted gold deposits of the Noranda cauldron, Rouyn-Noranda, Quebec, Canada: Unpublished Ph.D. thesis, Université de Montréal, Montréal, Canada, 318 p.

Selby, D., and Creaser, R.A., 2004, Macroscale NTIMS and microscale LA-MC-ICP-MS Re-Os isotopic analysis of molybdenite: Testing spatial restrictions for reliable Re-Os age determinations, and implications for the decoupling of Re and Os within molybdenite: *Geochimica et Cosmochimica Acta*, v. 68, p. 3897–3908.

Selby, D., Creaser, R.A., Stein, H.J., Markey, R.J., and Hannah, J.L., 2007, Assessment of the ^{187}Re decay constant by cross calibration of Re–Os molybdenite and U–Pb zircon chronometers in magmatic ore systems: *Geochimica et Cosmochimica Acta*, v. 71, p. 1999–2013.

Simard, M., Labbé, J.-Y., Maurice, C., Lacoste, P., Leclerc, A., and Boily, M., 2010, Synthesis of the Northeastern Superior Province: Ministère des Ressources naturelles et de la Faune, MM 2010-01, 188 p., 8 maps.

Sinclair, W.D., Jonasson, I.R., Kirkham, R.V., and Soregaroli, A.E., 2016, Rhenium in Canadian mineral deposits: Geological Survey of Canada, Open File 7780, 1 .zip file.

Smoliar, M.I., Walker, R.J., and Morgan, J.W., 1996, Re-Os ages of group IIA, IIIA, IVA, IVB iron meteorites: *Science*, v. 271, p. 1099–1102.

Taylor, B.E., de Kemp, E., Grunsky, E., Martin, L., Maxwell, G., Rigg, D., Goutier, J., Lauzière, K., and Dubé, B., 2014, Three-dimensional visualization of the Archean Horne and Quemont Au-bearing volcanogenic massive sulfide hydrothermal systems, Blake River Group, Quebec: *Economic Geology*, v. 109, p. 183–203.

Wilson, M.E., 1941, Noranda district, Quebec: Geological Survey of Canada, Memoir 229, 162 p.

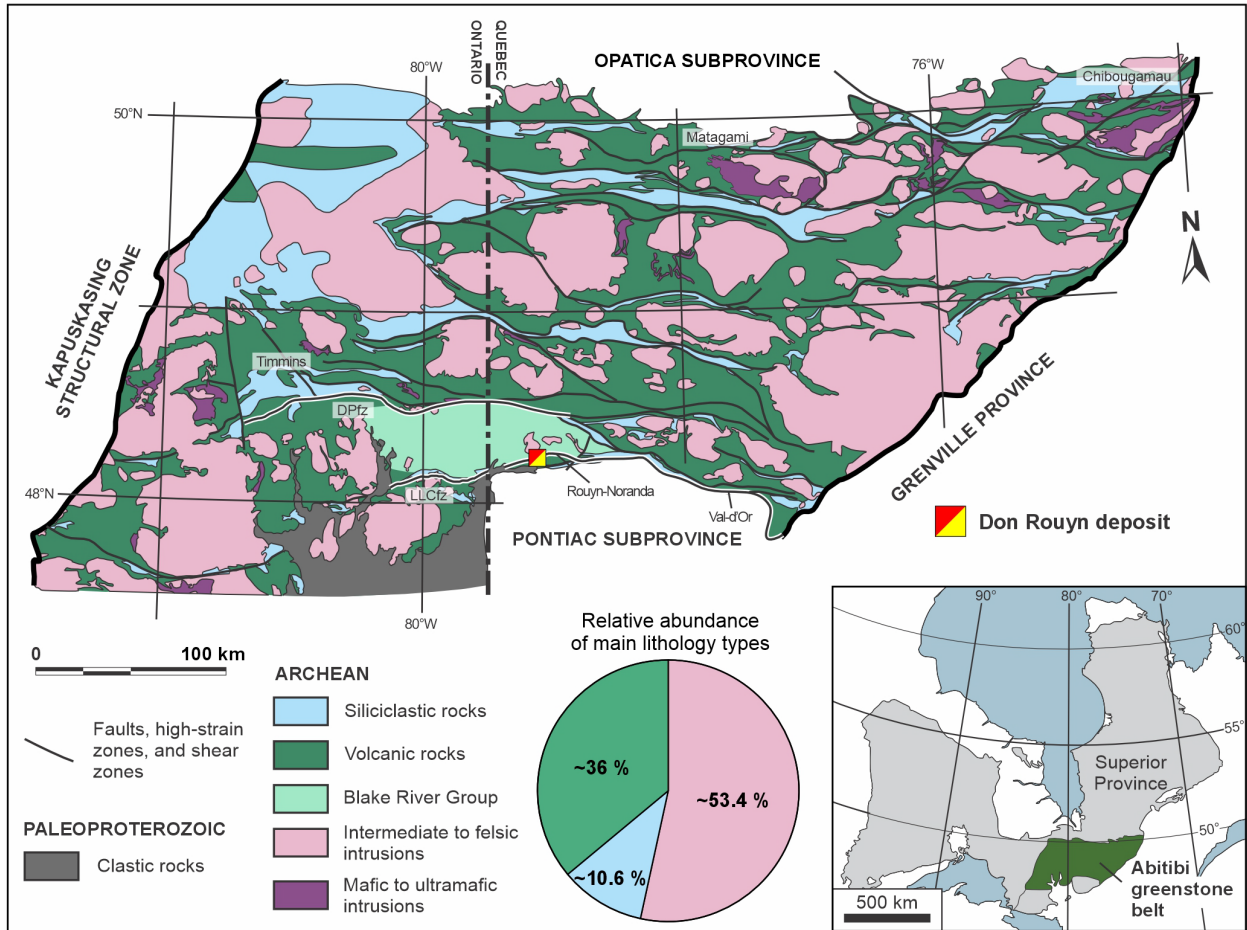


Figure 1. Geologic map of the Abitibi greenstone belt illustrating the distribution of volcanic, intrusive, and sedimentary rocks, as well as major structures (modified from McNicoll et al., 2014). The location of the Don Rouyn deposit, situated in the Blake River Group, is also shown. Pie chart with relative abundance of the main lithology types is from Mercier-Langevin et al. (2022). Inset shows location of the belt with respect to the Superior province. LLCfz = Larder Lake and Cadillac faults, DPfz = Destor-Porcupine fault zone.

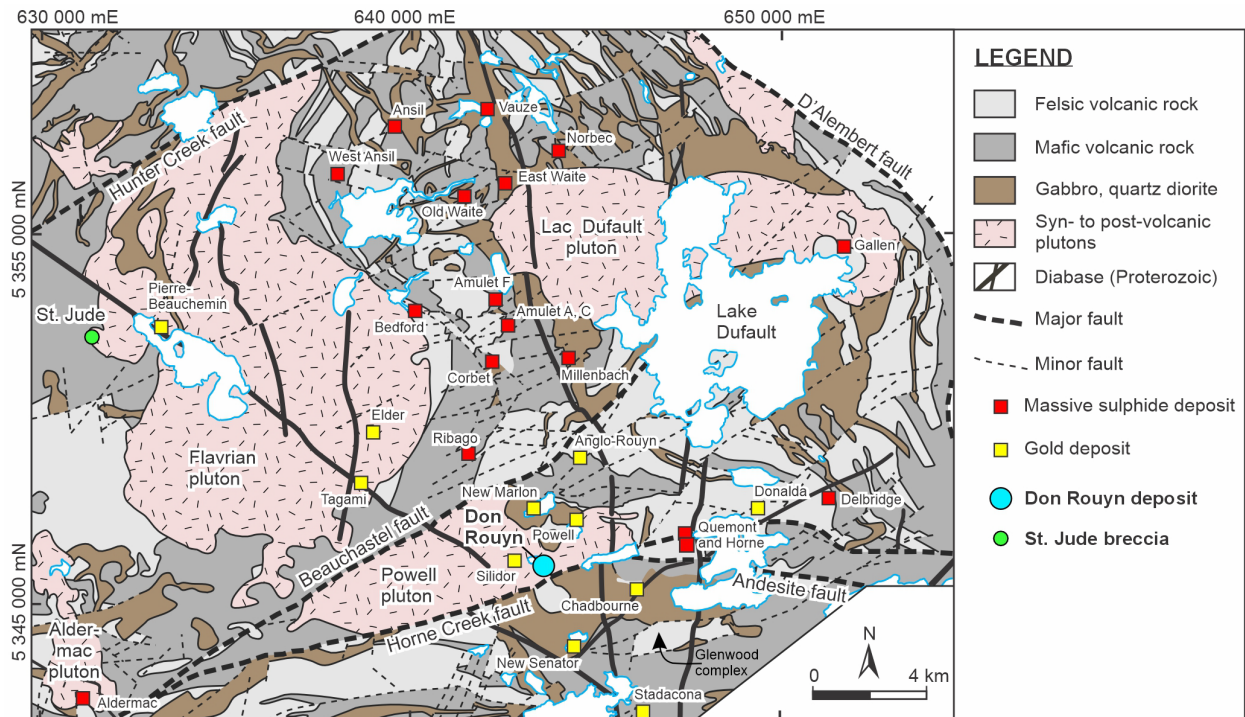


Figure 2. Simplified geologic map of the eastern portion of the Blake River Group (Modified from Système d'information géominère du Québec, and Monecke et al., 2017b) showing the location of the Don Rouyn deposit and St. Jude breccia showing, as well as volcanogenic massive sulphide and orogenic gold deposits in the area. UTM NAD83 Zone 17 coordinates.

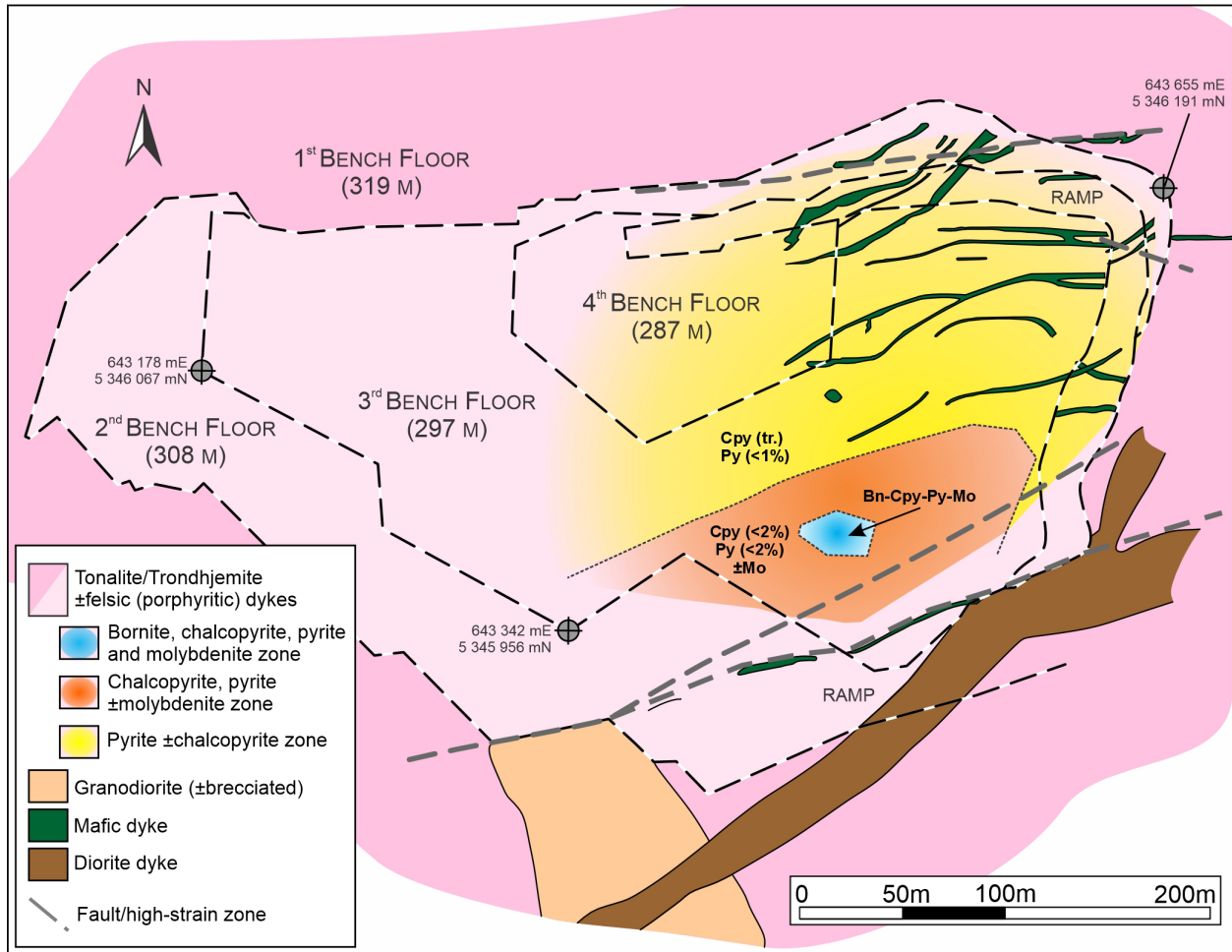


Figure 3. Simplified surface geologic map of the former Don Rouyn open pit mine. Redrawn from Goldie et al. (1979) and Jébrak et al. (1996). The map shows part of the Powell sunvolcanic pluton tonalite (trondhjemite) that hosts the Cu(-Au-Mo) zones that were historically mined primarily for siliceous flux material for the Horne smelter. UTM NAD83 Zone 17 coordinates.

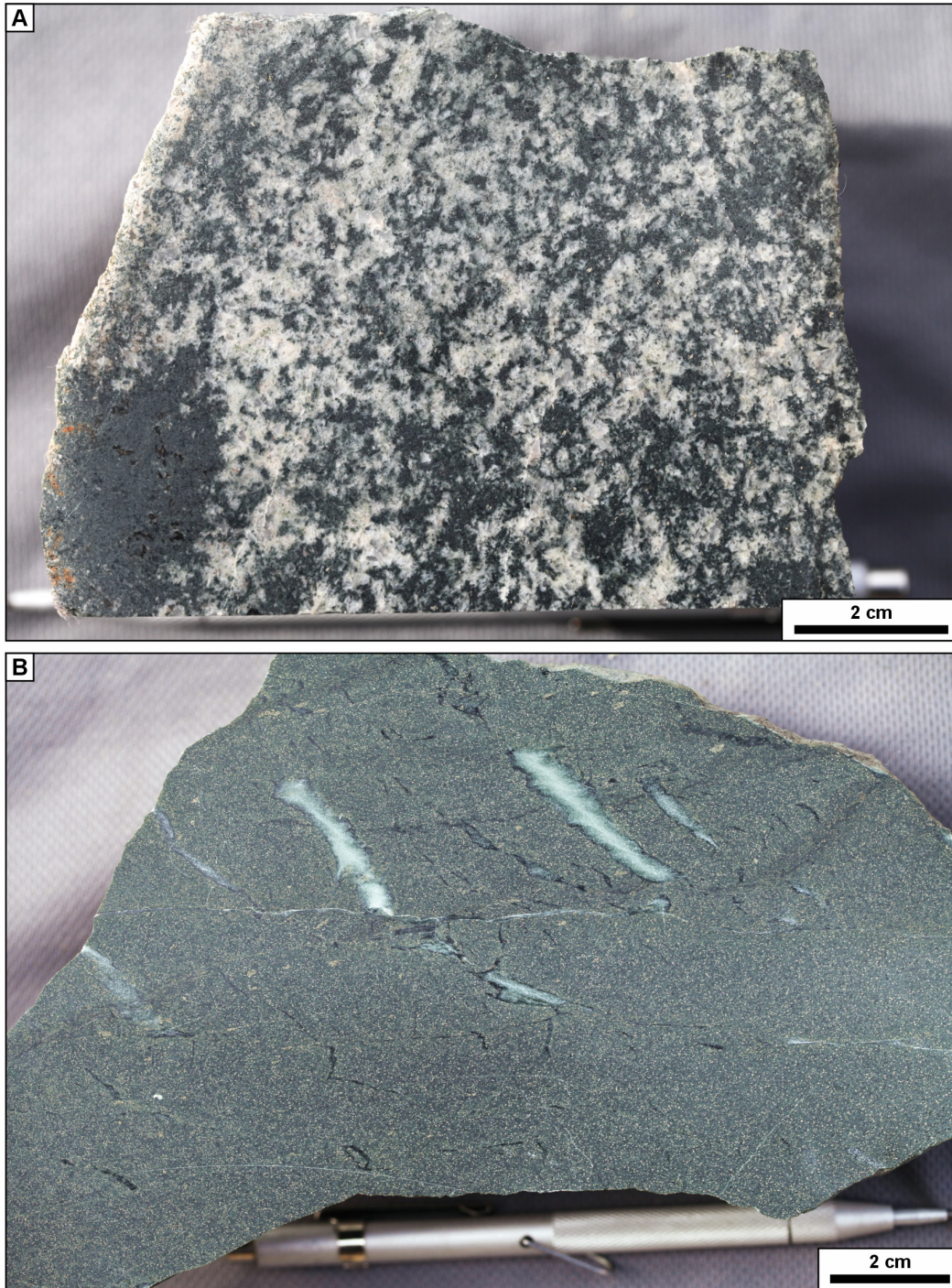


Figure 4. **A.** Example of least-altered Powell tonalite, unknown sample number, from GSC archives. Photograph by P. Mercier-Langevin, NRCan photo 2023-365. **B.** Sample from an altered, fine-grained mafic dyke that cuts the Powell pluton tonalite at the Don Rouyn mine, unknown sample number, from the GSC archives. Photograph by P. Mercier-Langevin, NRCan photo 2023-366.

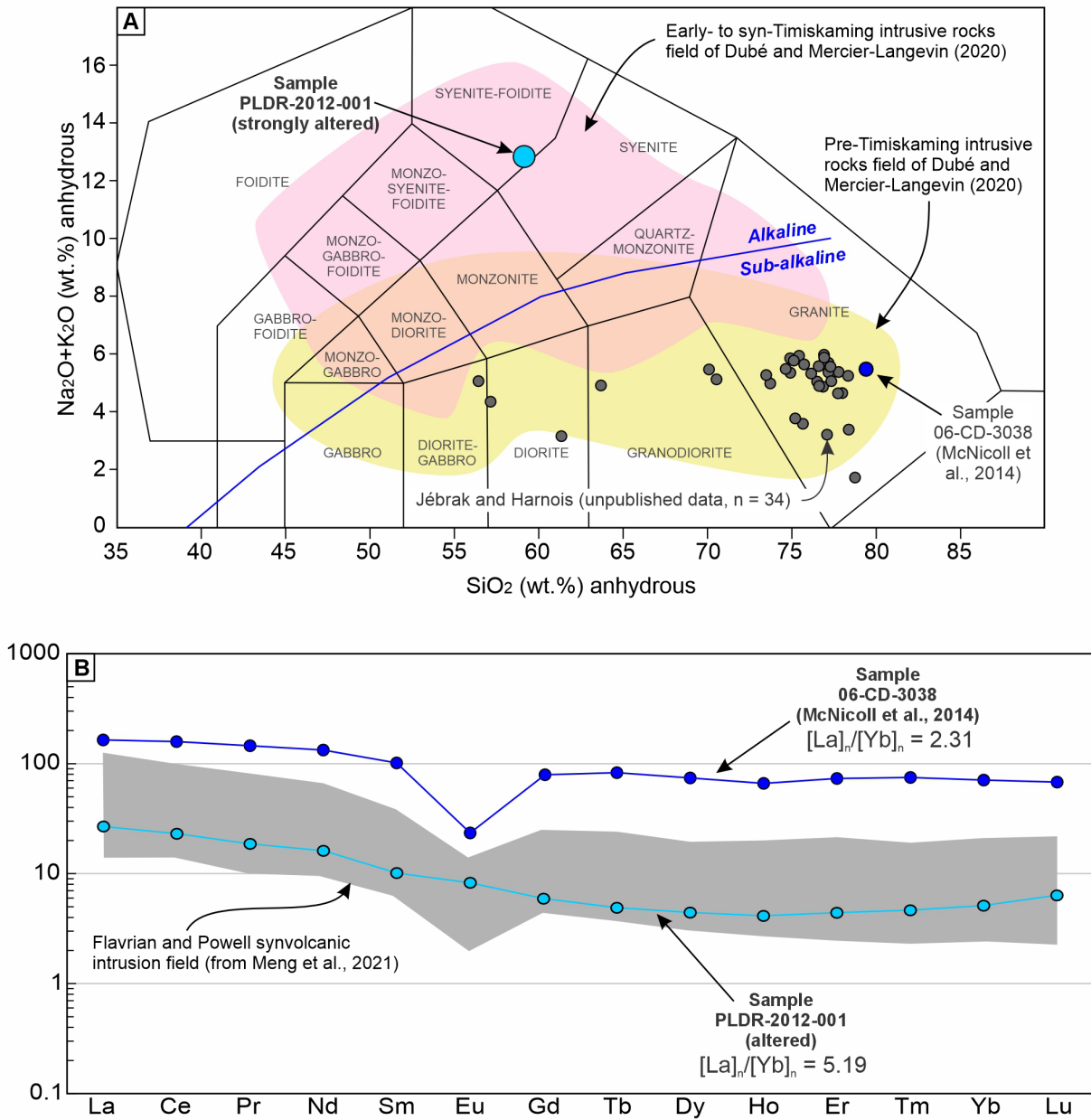


Figure 5. A. Total alkali silica classification diagram for magmatic rocks from Middlemost (1994). The diagram is calibrated for fresh rocks, and sample PLDR-2012-001 is from the mineralized and altered part of the Powell pluton at the former Don Rouyn mine. The diagram also shows sample 06-CD-3038 (dated Powell intusin sample) from McNicoll et al. (2014), and least-altered to mineralized samples from Jébrak and Harnois (unpublished). **B.** Rare-earth elements diagram, normalized on C1 chondrite values from McDonough and Sun (1995). Grey field from Meng et al. (2021) showing the range of REE signatures for the Flavrian intrusion. The diagram also shows the REE profile for sample 06-CD-3038 (dated Powell intusin sample) from McNicoll et al. (2014).

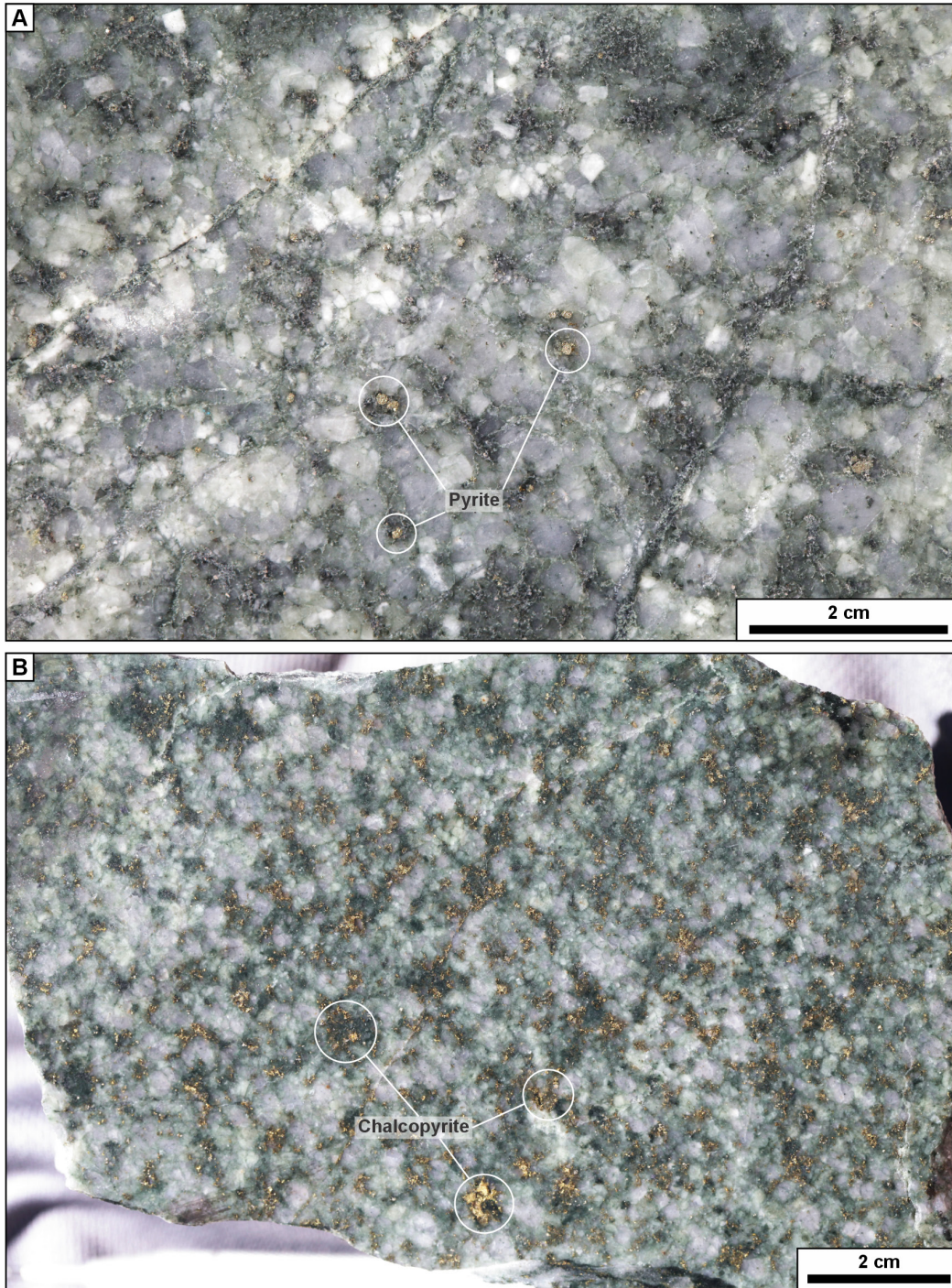


Figure 6. **A.** Chlorite, albite, epidote and carbonate-altered tonalite from the pyrite \pm chalcopyrite zone. GSC archive sample SYA-78-104-6, central part of open pit. Photograph by P. Mercier-Langevin, NRCan photo 2023-367. **B.** Chlorite, epidote, albite and carbonate-altered and mineralized tonalite from the chalcopyrite, pyrite \pm molybdenite zone, central part of open pit. GSC archive sample KQ-72-254. Photograph by P. Mercier-Langevin, NRCan photo 2023-368.

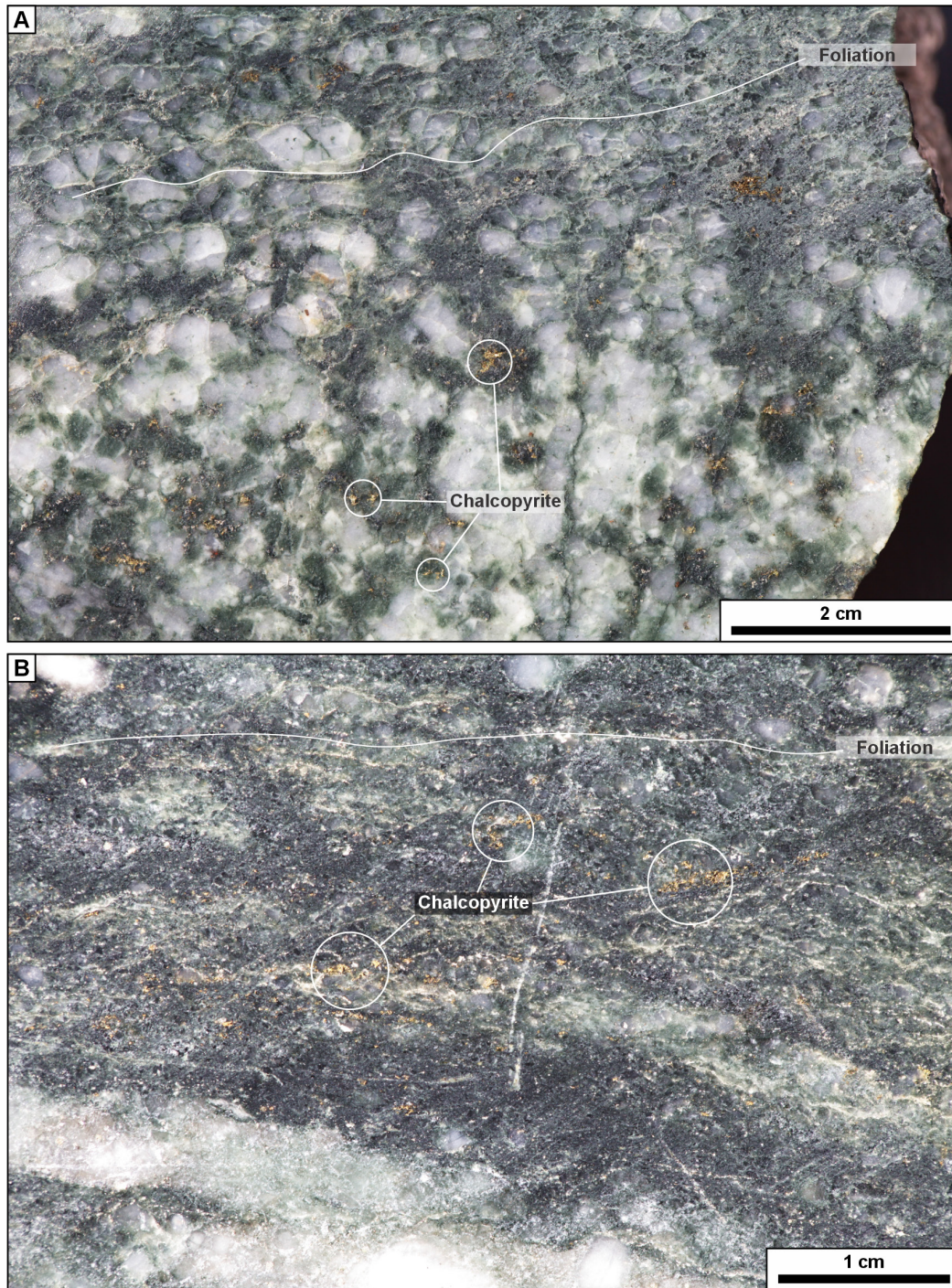


Figure 7. A. Chlorite-altered and foliated tonalite, chalcopyrite, pyrite \pm molybdenite zone, GSC archive sample SYA-78-104-5, central part of open pit. Photograph by P. Mercier-Langevin, NRCan photo 2023-369. **B.** Strongly chloritized and foliated band from the chalcopyrite, pyrite \pm molybdenite zone, central part of open pit, GSC archive sample KQ-72-258. Photograph by P. Mercier-Langevin, NRCan photo 2023-370.

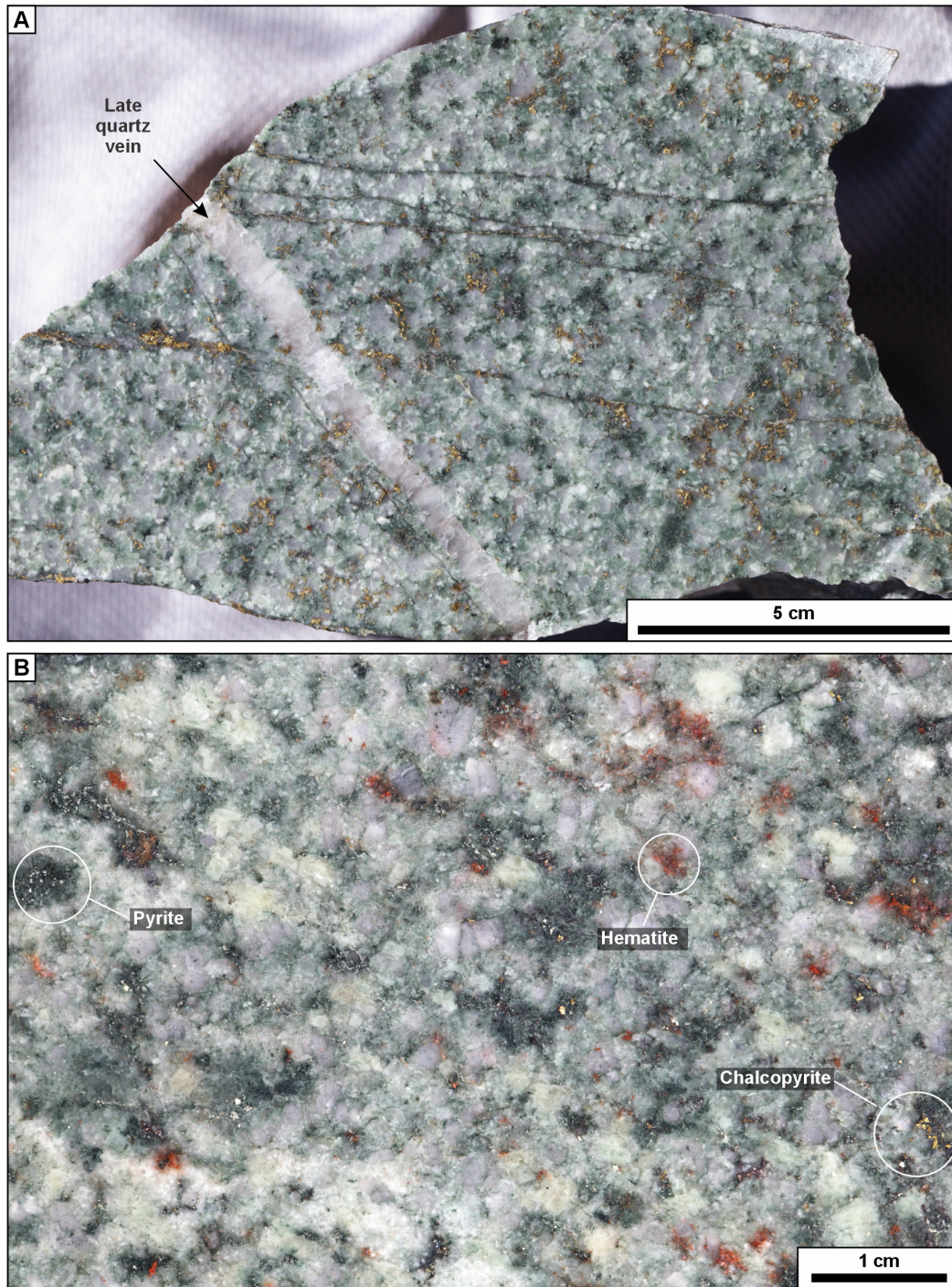


Figure 8. **A.** Chlorite, albite, epidote and carbonate-altered tonalite from the chalcopyrite, pyrite \pm molybdenite zone cut by a late quartz vein, GSC archive sample KQ-78-69. Photograph by P. Mercier-Langevin, NRCan photo 2023-371. **B.** Chlorite, epidote, albite, carbonate and hematite-altered tonalite from the pyrite \pm chalcopyrite zone, GSC archive sample KQ-72-252. Photograph by P. Mercier-Langevin, NRCan photo 2023-372.

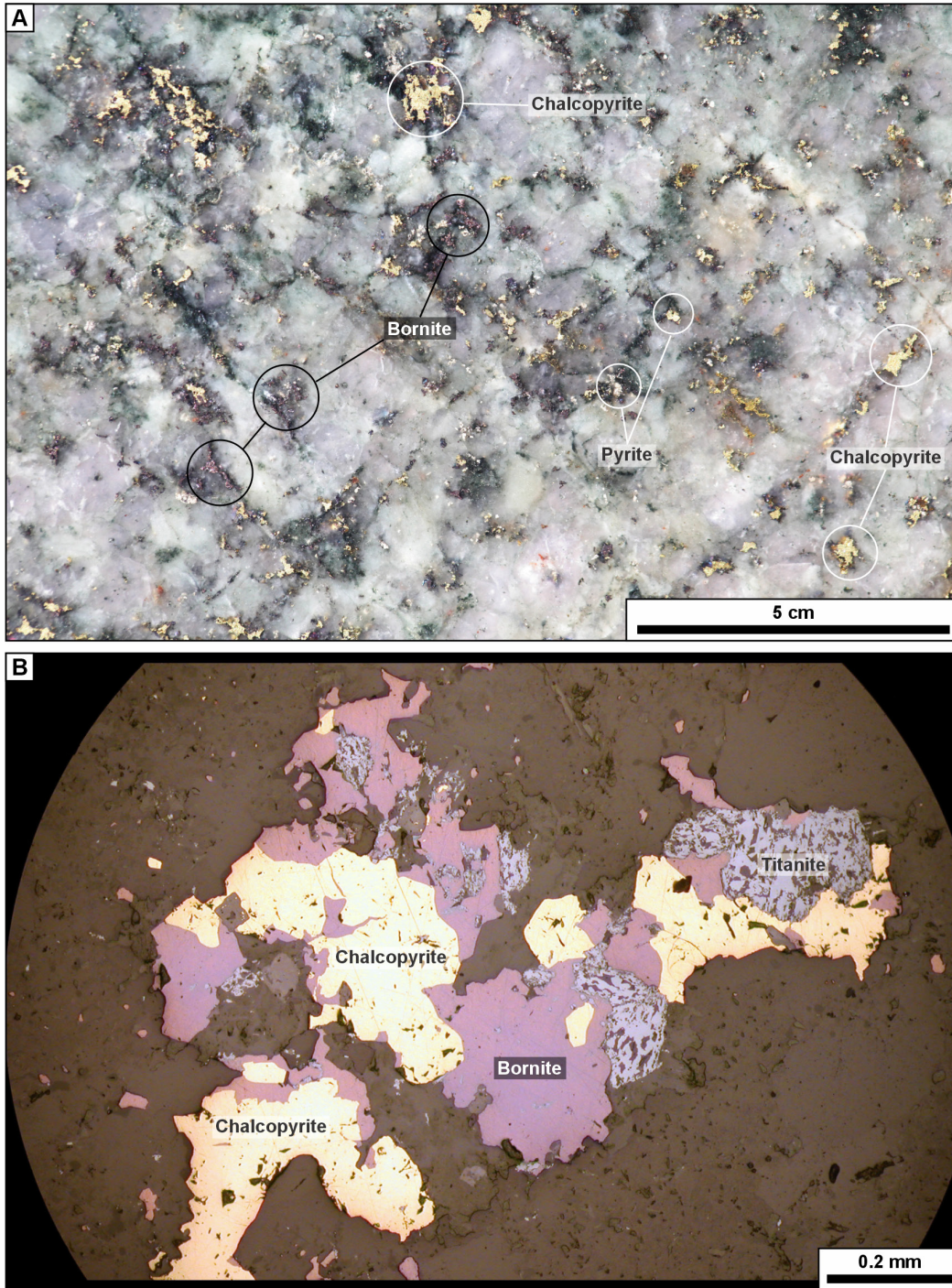


Figure 9. A. Disseminated bornite, chalcopyrite and pyrite zone, GSC archive sample KQ-72-253. Photograph by P. Mercier-Langevin, NRCan photo 2023-373. **B.** Photomicrograph (reflected light) of bornite and chalcopyrite intergrown with titanite, zircon and chlorite, sample PLDR-2012-001. Photograph by I. Kjarsgaard, NRCan photo 2023-374.

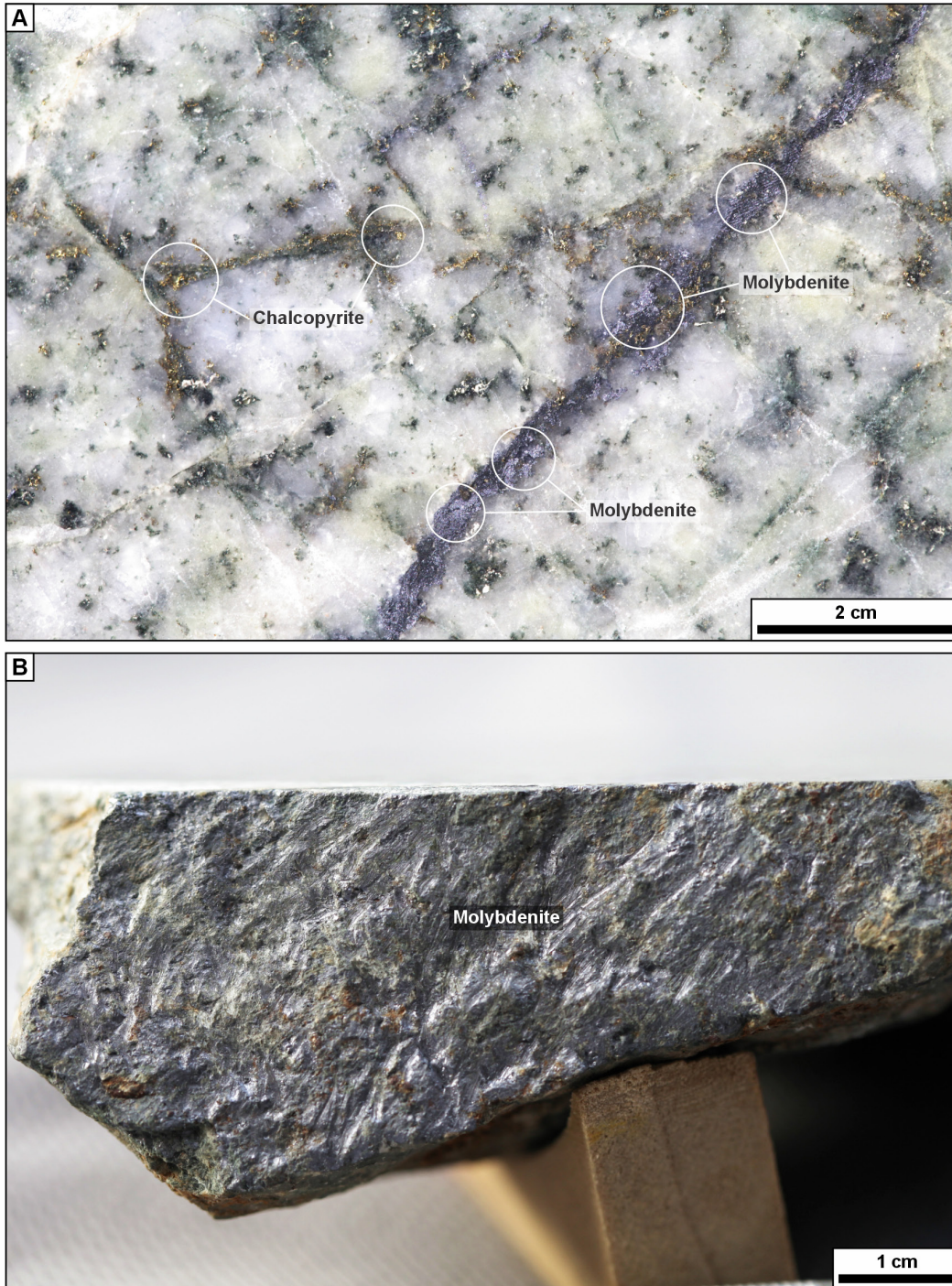


Figure 10. **A.** Molybdenite-chalcopyrite vein in the bornite, chalcopyrite and pyrite zone, GSC archive sample KQ-72-253. Photograph by P. Mercier-Langevin, NRCan photo 2023-375. **B.** Molybdenite-coated fracture/minor fault plane in the bornite, chalcopyrite and pyrite zone, unknown sample number, GSC archive. Photograph by P. Mercier-Langevin, NRCan photo 2023-376.

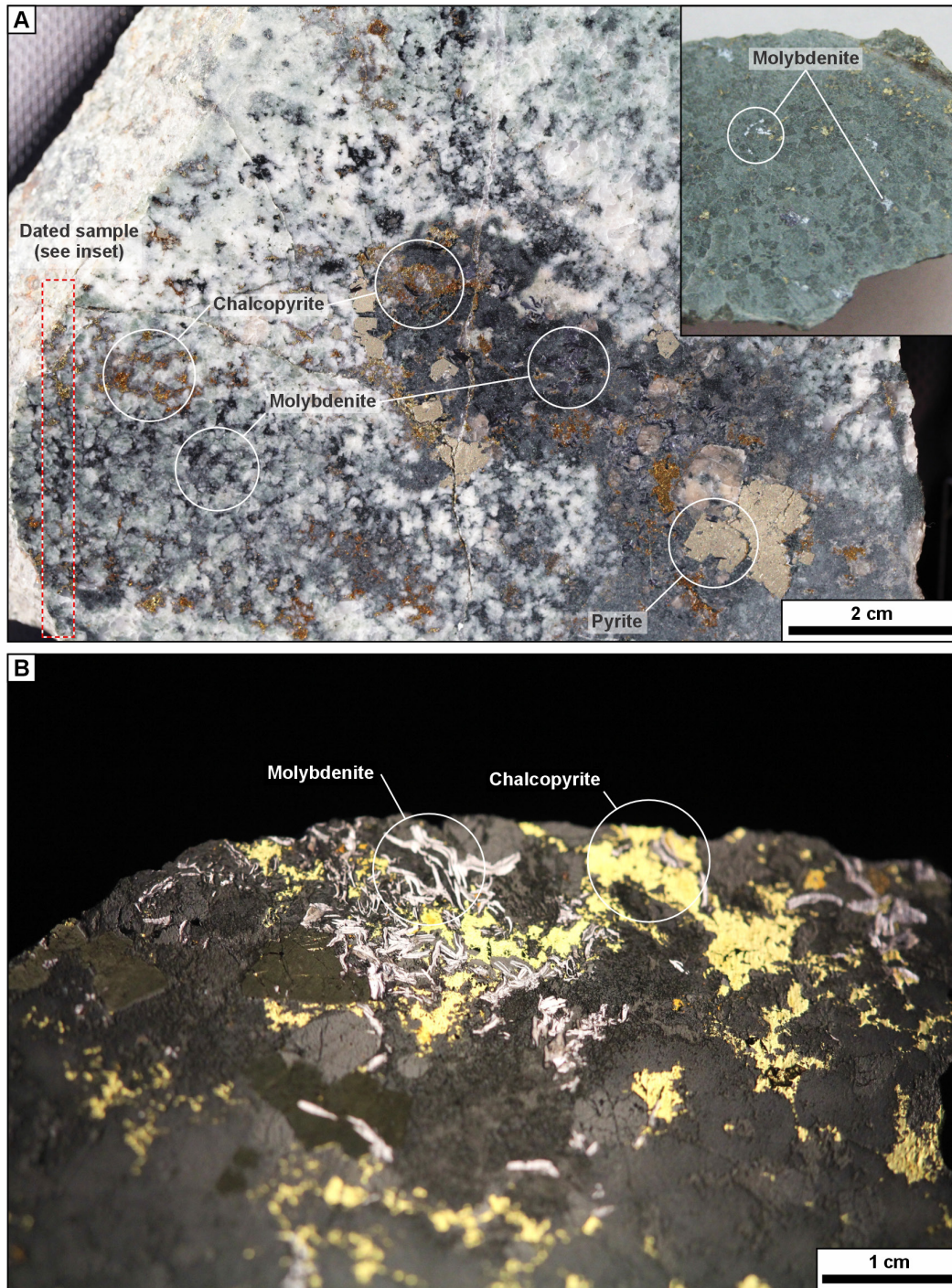


Figure 11. A. Molybdenite-rich sample from the bornite, chalcopyrite and pyrite zone, GSC archive sample JH-98-DR. Photograph by P. Mercier-Langevin, NRCan photo 2023-377. Inset: dated sample with disseminated molybdenite in a chlorite- and -albite-rich part of sample JH-98-DR. Photograph by R. Creaser, NRCan photo 2023-378. **B.** Abundant and coarse-grained molybdenite and chalcopyrite, GSC archive sample JH-98-DR. Photograph by P. Mercier-Langevin, NRCan photo 2023-379.

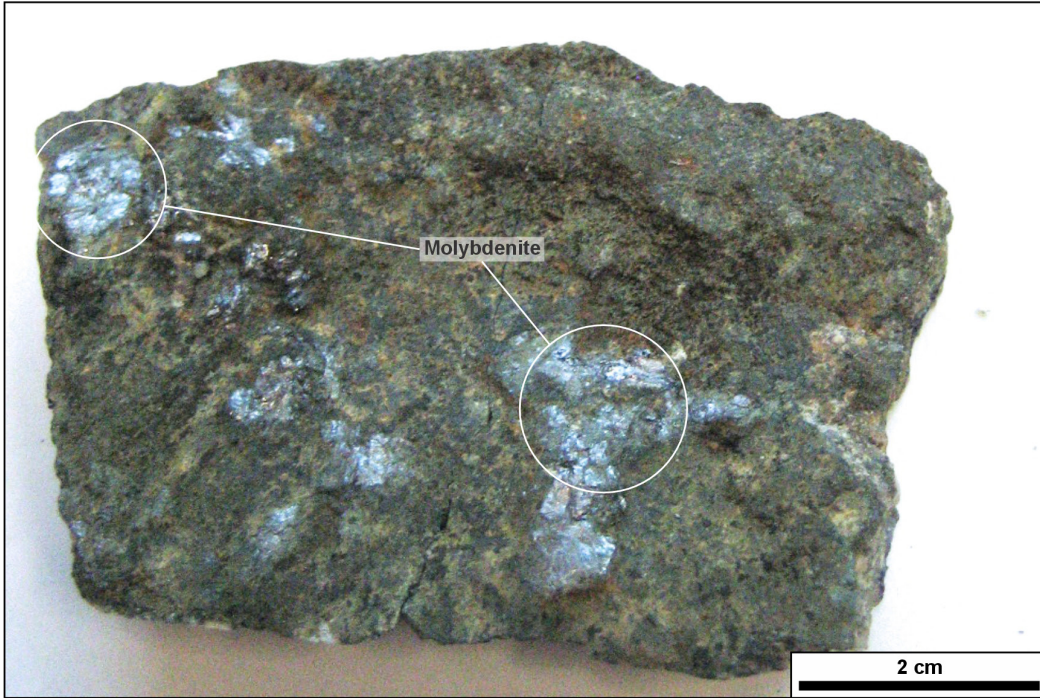


Figure 12. Abundant molybdenite along fractures, St. Jude sample, Sylvie showing (St. Jude breccia). Photograph by R. Creaser, NRCan photo 2023-380.

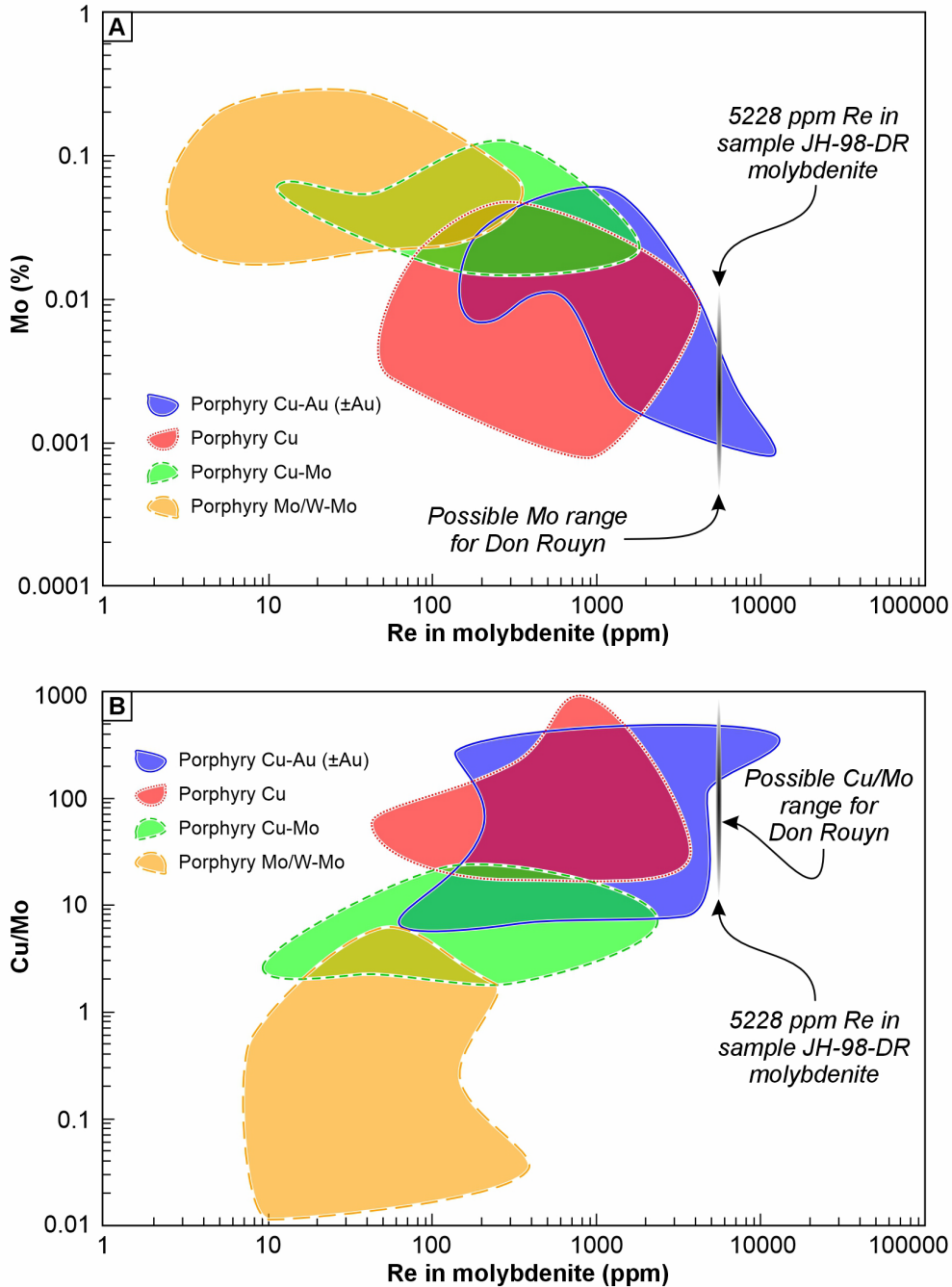


Figure 13. Diagrams comparing the composition of Canadian and foreign porphyry type deposits (from Sinclair et al., 2016). **A.** Plot of average content of molybdenite versus Mo grade (fields from Sinclair et al., 2016), showing the possible range for Don Rouyn deposit based on the Re content of dated sample JH-98-DR. **B.** Plot of average Re content of molybdenite versus average Cu/Mo ratio (fields from Sinclair et al., 2016), showing the possible range for Don Rouyn deposit based on the Re content of dated sample JH-98-DR.

Table 1. Re-Os isotopic results, mixed double $^{185}\text{Re}+^{190}\text{Os}+^{188}\text{Os}$ spike

Sample	Fraction	Weight	Re		^{187}Re		^{187}Os		Model		
			ppm	2σ	ppm	2σ	ppb	2σ	age (Ma)	2σ	2σ with λ
JH-98-DR	(Don Rouyn former mine: UTM NAD83 Zone 17: 643 460 mE, 5 345 990 mN (± 20 m))										
run 1	5 mg	5228	14	3286	9	150570	108	2689	7.0	11.0	
"St. Jude" sample	(Sylvie showing: UTM NAD 83 Zone 17: 631 700 mE, 5 352 151 mN)										
run1	36 mg	1.212	0	0.762	0	36.22	0	2789	7.0	12.0	
replicate 1	34 mg	1.170	0	0.735	0	34.74	0	2771	7.0	12.0	
replicate 2	17 mg	1.381	0	0.868	0	39.16	0.1	2648	7.0	12.0	
replicate 3	107 mg	1.293	0	0.813	0	37.69	0	2720	7.0	11.0	

ppb = parts per billion

ppm = parts per million

All uncertainties quoted at 2σ level of precisionAge uncertainty includes ^{187}Re decay constant uncertainty

Table 2. Chemical composition of sample PLDR-2012-001⁽¹⁾ (Powell pluton tonalite at the Don Rouyn mine).

Analyte Symbol	Unit Symbol	Detection Limit	PLDR-2012-001 ⁽²⁾
SiO ₂	%	0.01	58.5
Al ₂ O ₃	%	0.01	21.74
Fe ₂ O ₃	%	0.01	0.94
FeO	%	0.1	2.1
MnO	%	0.001	0.055
MgO	%	0.01	0.73
CaO	%	0.01	1.71
Na ₂ O	%	0.01	8.69
K ₂ O	%	0.01	4.03
TiO ₂	%	0.001	0.134
P ₂ O ₅	%	0.01	0.07
Total S	%	0.01	0.02
CO ₂	%	0.01	0.15
LOI	%		0.38
Total	%	0.01	99.32
Zr	ppm	1	60
Y	ppm	0.5	5.6
Nb	ppm	0.2	1.5
Hf	ppm	0.1	1.1
Ta	ppm	0.01	0.05
Th	ppm	0.05	0.92
U	ppm	0.01	0.42
Ba	ppm	2	96
Rb	ppm	1	51
Sr	ppm	2	92
Sc	ppm	1	9
Li	ppm	1	33
Be	ppm	1	<1
B	ppm	1	24
V	ppm	5	84
Cr	ppm	1	6
Co	ppm	0.5	6.1
Ni	ppm	1	2
Cu	ppm	0.5	38.4
Zn	ppm	0.5	41.0
Pb	ppm	2	6
Cd	ppm	0.2	<0.2
Ga	ppm	1	23
Ge	ppm	0.5	1.1
Au	ppb	5	8
Ag	ppm	0.5	6.1
As	ppm	0.1	<0.1
Sb	ppm	0.02	<0.02
Hg	ppb	5	<5
Bi	ppm	0.02	<0.05
Tl	ppm	0.05	0.52
Se	ppm	0.1	<1
Te	ppm	0.02	0.01
Sn	ppm	1	<1
W	ppm	0.5	<0.5
Mo	ppm	1	<1
Cs	ppm	0.1	1.1
In	ppm	0.1	<0.1
Mn	ppm	2	375

Table 2. Chemical composition of sample PLDR-2012-001⁽¹⁾ (Powell pluton tonalite at the Don Rouyn mine).

Analyte Symbol	Unit Symbol	Detection Limit	PLDR-2012-001 ⁽²⁾
La	ppm	0.05	6.42
Ce	ppm	0.05	14.3
Pr	ppm	0.01	1.75
Nd	ppm	0.05	7.47
Sm	ppm	0.01	1.52
Eu	ppm	0.005	0.472
Gd	ppm	0.01	1.20
Tb	ppm	0.01	0.18
Dy	ppm	0.01	1.11
Ho	ppm	0.01	0.23
Er	ppm	0.01	0.72
Tm	ppm	0.005	0.117
Yb	ppm	0.01	0.84
Lu	ppm	0.002	0.159

⁽¹⁾ Sample courtesy of Ministère des Ressources naturelles et des Forêts.

⁽²⁾ Sample from the Cu-rich zone, strongly altered, although not mineralized

Analytical methods

Whole-rock analyses were performed at Activation Laboratories Ltd. in Ancaster, Ontario, using a combination of their standard preparation and analytical packages, the details of which can be found at <https://actlabs.com/geochemistry/litho-geochemistry-and-whole-rock-analysis>.

Samples were initially dried (60°C) and crushed to at least 90% (<2mm) in a steel jaw crusher. A mechanically split fraction was pulverized in a chromium-free steel mill until 95% of the sample material passed through a 74 µm mesh. Major elements were determined by lithium metaborate-tetraborate fusion followed by inductively coupled plasma mass spectrometry (ICP-MS; FUS-MS). Trace and rare earth elements were determined by a combination of lithium metaborate-tetraborate and total digestion (four acids) followed by inductively coupled plasma mass spectrometry (ICP-MS; FUS-MS) and inductively coupled plasma atomic emission spectrometry (ICP-OES; FUS-ICP). FeO was determined by titration using a cold acid digestion (ammonium metavanadate and hydrofluoric acid) in an open system (TITR).

For chalcophile elements a four-acid digestion ICP-MS (TD-MS) method was preferred. Aqua regia (AR-MS) digestion coupled with ICP-MS was chosen to analyze As, Sb, Bi, Se and Te. Boron was determined by gamma neutron activation analysis (PGNAA). Gold and silver were measured by a combination of atomic absorption (FA-AA), fire assay, and gravimetry (FA-GRAV). High-grade ore zone samples were re-analyzed with a combination of fire assay and gravimetric methods for gold and silver (FA-GRAV) and aqua regia dissolution (ICP-OES) or sodium peroxide fusion (FUS-Na2O2) with ICP-OES depending on the analyte. CO2 and Total (S) were determined by combustion infrared analysis (IR). Fluorine was determined by lithium metaborate and tetraborate fusion and fluoride ion electrode analysis (FUS-ISE). Chlorine was determined by instrumental neutron activation analysis (INAA). Mercury was determined by cold vapour flow injection (FIMS) following aqua regia digestion.

Table 3. Petrographic description and mineralogy of mineralized samples from the Don Rouyn mine.

Sample	Mineralogy ⁽¹⁾ (relative abundance, in %)																				
	Qz	Ab	Sr	Cal	Chl	Czo	Ep	Tur	Rt	Zrn	Xtm	Aln	Ap	Pst/Syn	Ccp	Bn	Mol	Py	Cv	Dg	Au-Ag
PLDR-2012-001	44	44	10	tr.	2			tr.	tr.	tr.	tr.		tr.			tr.	tr.	tr.		tr.	tr.
JH-98-DR ⁽²⁾	20	38	1	8	17	4				tr.	tr.		tr.	2		8		1	tr.		
KQ-78-68A	60	20	9	tr.	10		tr.		tr.	tr.			tr.		tr.			tr.			
KQ-72-249	43	47	5	1	2			tr.	tr.	tr.			tr.	tr.		2	tr.				
SYA-78-103	40	48	10	tr.	2				tr.	tr.	tr.	tr.	tr.			tr.				tr.	tr.

⁽¹⁾ Mineral name abbreviations: Ab = albite, Aln = allanite, Ap = apatite, Bn = bornite, Cal = calcite, Ccp = chalcopyrite, Chl = chlorite, Cv = covellite, Czo = clinoisite, Ep = epidote, Pst = parisite, Py = pyrite, Qz = quartz, Rt = rutile, Sr = sericite, Syn = synchisite, Tur = turmaline, Xtm = xenotime, Zrn = zircon, tr = traces.

⁽²⁾ Dated sample (Re-Os on molybdenite)

Sample	Petrographic description
PLDR-2012-001	Fine to medium grained assemblage consisting of altered euhedral plagioclase (now albite) and blocky quartz in about equal amounts, with minor interstitial patches containing green chlorite ± rutile + sulphides and permeated by veinlets of sericite ± chlorite. The feldspar is overprinted by fine grained sericite and trace chlorite and carbonate. Sulphides consist of anhedral chalcopyrite intergrown with about equal amounts of bornite, which are associated with chlorite and trace carbonate. Fine grained acicular aggregates of dark brown subhedral rutile occur in the chlorite patches. The quartz is blocky, anhedral with slightly serrated edges and contains abundant inclusions trails, suggesting it might be of hydrothermal origin.
JH-98-DR ⁽²⁾	Hydrothermally altered and mineralized quartz-feldspar assemblage containing coarse chalcopyrite, molybdenite and euhedral pyrite porphyroblasts. The bulk of the rock consists of fine to medium grained slightly chlorite-altered plagioclase laths intergrown with minor medium grained anhedral quartz (possibly partly primary and partly hydrothermal in origin). This assemblage is altered by intense green chlorite ± sericite and coarse radiating aggregates of clinoisite and calcite. Much of the clinoisite has been replaced by calcite. Sulphides consist of very fine to coarse anhedral chalcopyrite, coarse deformed molybdenite surrounding the clinoisite-carbonate aggregates, as well as a few discrete pyrite porphyroblasts, which are up to 3mm in diameter and show poikilitic cores and zoned rims. The chalcopyrite is marginally intergrown with carbonate, green chlorite, clinoisite and apatite. A late carbonate-filled vein cuts the entire assemblage.
KQ-78-68A	Quartz-feldspar-rich rock consisting of abundant quartz, which is anhedral, lobed to skeletal and intergrown with more or less altered feldspar (mostly albite) showing graphic intergrowth patterns in some areas, while in others the feldspar component has been heavily altered by sericite-chlorite ± carbonate and the quartz component appears like grain fragments floating in a foliated and slightly crenulated chlorite-sericite matrix. Rare remnants of primary opaques appear as diffuse grids of ilmenite-rutile lamellae or fine grained aggregates of rutile in chlorite. This felsic assemblage has been impregnated with green chlorite and chalcopyrite which appear as random patches and disseminations. Chlorite appears to have replaced rare primary biotite and seems to be mostly of hydrothermal origin.
KQ-72-249	Abundant quartz is intergrown with abundant euhedral to subhedral sericite-altered feldspar (mostly plagioclase). The assemblage is invaded by green chlorite + chalcopyrite ± trace bornite occurring mostly interstitially. The chlorite-chalcopyrite patches also host dark aggregates of rutile (leucosene), remnants of former opaques. Fine grained anhedral apatite is associated with rutile aggregates in chlorite-chalcopyrite. Minor fine grained clear potassium feldspar is intergrown with chalcopyrite in the chlorite patches.
SYA-78-103	Coarse subhedral to anhedral quartz, coarse plagioclase set in a medium grained quartz-plagioclase matrix. The larger feldspars are more strongly sericite-altered than the groundmass plagioclase. Patches of chlorite intergrown with anhedral chalcopyrite, subhedral pyrite ± carbonate occur interstitially. Fine grained dark rutile aggregates in chlorite represent remnants of altered primary FeTi-oxides. Zircon and allanite occur as fine grained accessory minerals in chlorite.